

**An Experimental and Analytical Study
of Timber Bridges Comprised of
Longitudinal Stringers, Transverse Decking,
and Diaphragms**

Final Report

**Michael Accorsi, Associate Professor
Scott Anderson, Graduate Assistant
University of Connecticut**

JHR 93-217

March 1993

Disclaimer

This research was sponsored by the Joint Highway Research Advisory Council (JHRAC) of the University of Connecticut and the Connecticut Department of Transportation and was carried out in the Civil Engineering Department of the University of Connecticut.

The contents of this report reflect the views of the authors who are responsible for the facts and accuracy of the data presented herein. The contents do not necessarily reflect the official views or policies of the University of Connecticut or the Connecticut Department of Transportation. This report does not constitute a standard, specification, or regulation.

1. Report No. JHR 93-217		2. Government Accession No.		3. Recipient's Catalog No.	
4. Title and Subtitle An Experimental and Analytical Study of Timber Bridges Comprised of Longitudinal Stringers, Transverse Decking, and Diaphragms				5. Report Date March 5, 1993	
				6. Performing Organization Code	
7. Author(s) Michael L. Accorsi and Scott T. Anderson				8. Performing Organization Report No. JHR 93-217	
9. Performing Organization Name and Address University of Connecticut Department of Civil Engineering 191 Auditorium Road, Box U-37 TI Storrs, CT 06269				10. Work Unit No. (TRAIS)	
				11. Contract or Grant No.	
12. Sponsoring Agency Name and Address Connecticut Department of Transportation 280 West Street Rocky Hill, CT 06067-0207				13. Type of Report and Period Covered Final Report	
				14. Sponsoring Agency Code	
15. Supplementary Notes					
16. Abstract An experimental and analytical study was performed on a timber bridge comprised of longitudinal stringers, transverse decking, and diaphragms. The objective was to develop a new type of timber bridge that would better utilize native timber species and other local resources that could be used for longer spans. The structural response of three laminated bridge deck specimens was measured experimentally and the feasibility of these decks for actual construction was evaluated. A small scale model of the bridge was constructed and tested to investigate the structural behavior of the proposed bridge. The influence of diaphragms on the overall behavior was found to be significant. A finite element model of the proposed bridge was developed to further investigate the bridge behavior. Results from the finite element model are compared to relevant design specifications.					
17. Key Words Timber Bridges, Laminated Bridge Deck, Diaphragms, Finite Element Model			18. Distribution Statement No Restrictions		
19. Security Classif. (of this report) Unclassified		20. Security Classif. (of this page) Unclassified		21. No. of Pages 45	22. Price

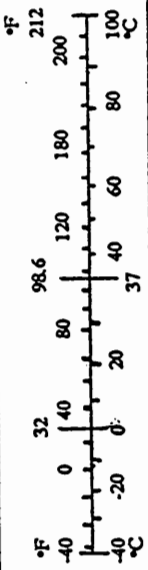
Acknowledgements

The authors gratefully acknowledge support from The University of Connecticut Research Foundation for the experimental program conducted as part of this project. The authors would also like to thank Dywidag Systems International (Lincoln Park, NJ), Berlin Steel, and Blakeslee Prestress for donating materials used in the experimental program.

SI* (MODERN METRIC) CONVERSION FACTORS

APPROXIMATE CONVERSIONS TO SI UNITS				APPROXIMATE CONVERSIONS TO SI UNITS			
Symbol	When You Know	Multiply By	To Find	Symbol	When You Know	Multiply By	To Find
<u>LENGTH</u>				<u>LENGTH</u>			
in	inches	25.4	millimetres	mm	millimetres	0.039	inches
ft	feet	0.305	metres	m	metres	3.28	feet
yd	yards	0.914	metres	m	metres	1.09	yards
mi	miles	1.61	kilometres	km	kilometres	0.621	miles
<u>AREA</u>				<u>AREA</u>			
in ²	square inches	645.2	millimetres squared	mm ²	millimetres squared	0.0016	square inches
ft ²	square feet	0.093	metres squared	m ²	metres squared	10.764	square feet
yd ²	square yards	0.836	metres squared	m ²	hectares	2.47	acres
ac	acres	0.405	hectares	ha	kilometres squared	0.386	square miles
mi ²	square miles	2.59	kilometres squared	km ²			
<u>VOLUME</u>				<u>VOLUME</u>			
fl oz	fluid ounces	29.57	millilitres	mL	millilitres	0.034	fluid ounces
gal	gallons	3.785	Litres	L	litres	0.264	gallons
ft ³	cubic feet	0.028	metres cubed	m ³	metres cubed	35.315	cubic feet
yd ³	cubic yards	0.765	metres cubed	m ³	metres cubed	1.308	cubic yards
<u>MASS</u>				<u>MASS</u>			
oz	ounces	28.35	grams	g	grams	0.035	ounces
lb	pounds	0.454	kilograms	kg	kilograms	2.205	pounds
T	short tons (2000 lb)	0.907	megagrams	Mg	megagrams	1.102	short tons (2000 lb)
<u>TEMPERATURE (exact)</u>				<u>TEMPERATURE (exact)</u>			
°F	Fahrenheit temperature	5(F-32)/9	Celcius temperature	°C	Celcius temperature	1.8C + 32	Fahrenheit temperature

NOTE: Volumes greater than 1000 L shall be shown in m³.



*SI is the symbol for the International System of Measurement

Table of Contents

Title Page, Disclaimer	i
Technical Report Documentation Page	ii
Acknowledgements.....	iii
Modern Metric Conversion Factors	iv
Table of Contents	v
List of Figures	vi
1.0 Introduction	1
1.1 Scope	1
2.0 Timber Bridge Deck Study	3
2.1 Test Results	5
2.2 Feasibility of Deck Construction	9
3.0 Bridge Model Tests	11
3.1 Test Results	11
4.0 Analysis of Timber Bridge Behavior	15
4.1 Analysis of Deck Forces	19
4.2 Analysis of Stringer Forces	23
5.0 Conclusions	30
References.....	34
Appendix A: Timber Bridge Design	35

List of Figures

- Figure 1. Timber Bridge with Longitudinal Stringers, Transverse Decking, and Diaphragms
- Figure 2. Test Configuration for Timber Panels
- Figure 3. Theoretical Load-Deflection Curves for Steel Dowels, Solid Wood Section, and Solid Wood Section with Dowels
- Figure 4. Lab Test of Bolted Deck Panel, (a) Load-Deflection Curve, (b) Bending Moment Carried by Steel Dowels
- Figure 5. Load-Deflection Curve for Stressed Deck Panels, (a) Dywidag Rods, (b) Prestressing Cable
- Figure 6. Normalized Stiffnesses of Deck Panels
- Figure 7. Testing Configuration used for Small Scale Bridge Model
- Figure 8. Load-Deflection Curve for Bridge Model
- Figure 9. Transverse Deflection of Bridge Model at Midspan without Diaphragms
- Figure 10. Transverse Deflection of Bridge Model at Midspan with Diaphragms
- Figure 11. Diaphragm to Stringer Connection
- Figure 12. Transverse Deflection of Bridge Model at Midspan with Welded Diaphragms and No Deck
- Figure 13. Timber Bridge and the Finite Element Model, (a) Three-Dimensional Bridge, (b) Two-Dimensional Finite Element Model
- Figure 14. Finite Element Models of Transverse Section, (a) Two-Dimensional Composite Model, (b) Two-Dimensional Noncomposite Model, (c) One-Dimensional Noncomposite Model
- Figure 15. Transverse Deflection of the Three Models
- Figure 16. Transverse Deflection of Bridge

- Figure 17. Primary Deck Forces, (a) Primary Moment,
(b) Primary Shear
- Figure 18. Secondary Deck Forces, (a) Secondary Moment,
(b) Secondary Shear
- Figure 19. Transverse Deflection of Bridge with Reduced
Stiffness
- Figure 20. Primary Deck Forces with Reduced Stiffness,
(a) Primary Moment, (b) Primary Shear
- Figure 21. Secondary Deck Forces with Reduced Stiffness,
(a) Primary Moment, (b) Primary Shear
- Figure 22. Truck Load Position, (a) Position to Produce
Maximum Moment, (b) Position on Finite Element
Model
- Figure 23. Stringer Forces Under Wheel Load, (a) Moment
Diagram, (b) Shear Diagram
- Figure 24. Transverse Deflection of the Bridge with and
without Diaphragms
- Figure 25. Primary Deck Moments with and without
Diaphragms
- Figure 26. Stringer Forces Opposite of Wheel Load,
(a) Moment Diagram, (b) Shear Diagram

An Experimental and Analytical Study of Timber Bridges Comprised of Longitudinal Stringers, Transverse Decking, and Diaphragms

1.0 Introduction

Modern timber bridges are a cost-effective bridge type for rural bridge replacements. The benefits of timber bridges are primarily derived from the use of native timber species and other local resources, such as local construction crews, sawmills, and preservative treatment plants. The most common type of timber bridge is constructed entirely of glue-laminated lumber which only partially utilizes local resources. Although glue-laminated bridges can be constructed by town crews, the laminating and fabrication are usually performed at a non-local facility using non-native species.

More recently, stress-laminated timber bridges have been developed that eliminate the need for glue-laminating and, therefore, allow for the use of native species. In this type of bridge, conventional sawn lumber is stressed together by steel rods to form a monolithic timber bridge deck. To date, only longitudinal stress-laminated timber bridges have been seriously developed and an AASHTO design guide was recently issued [1]. For this type of bridge, the superstructure consists of a single layer of stressed timbers and, therefore, the span obtainable for this design is limited by available lumber size. For example, assuming a 12 inch deck thickness, the approximate maximum span for an HS 20-44 loading is 26 feet [2]. An additional consideration with stress-laminated timber bridges is the loss of prestress due to wood creep.

In this study, the primary objective was to put forth a new type of timber bridge design that can better utilize native timber species and other local resources but was not limited to short spans. The design considered consists of glue-laminated timber stringers with steel diaphragms supporting a transverse timber deck as shown in Figure 1. This is a common design for glue-laminated timber bridges; however, in this study, the glue-laminated deck is replaced with either a bolted or stressed timber deck made from a native species. Eastern Hemlock is an abundant and inexpensive native species that was chosen as the deck material.

1.1 Scope

In this study, the structural behavior of timber bridges consisting of glue-laminated timber stringers with steel diaphragms supporting a transverse timber deck is

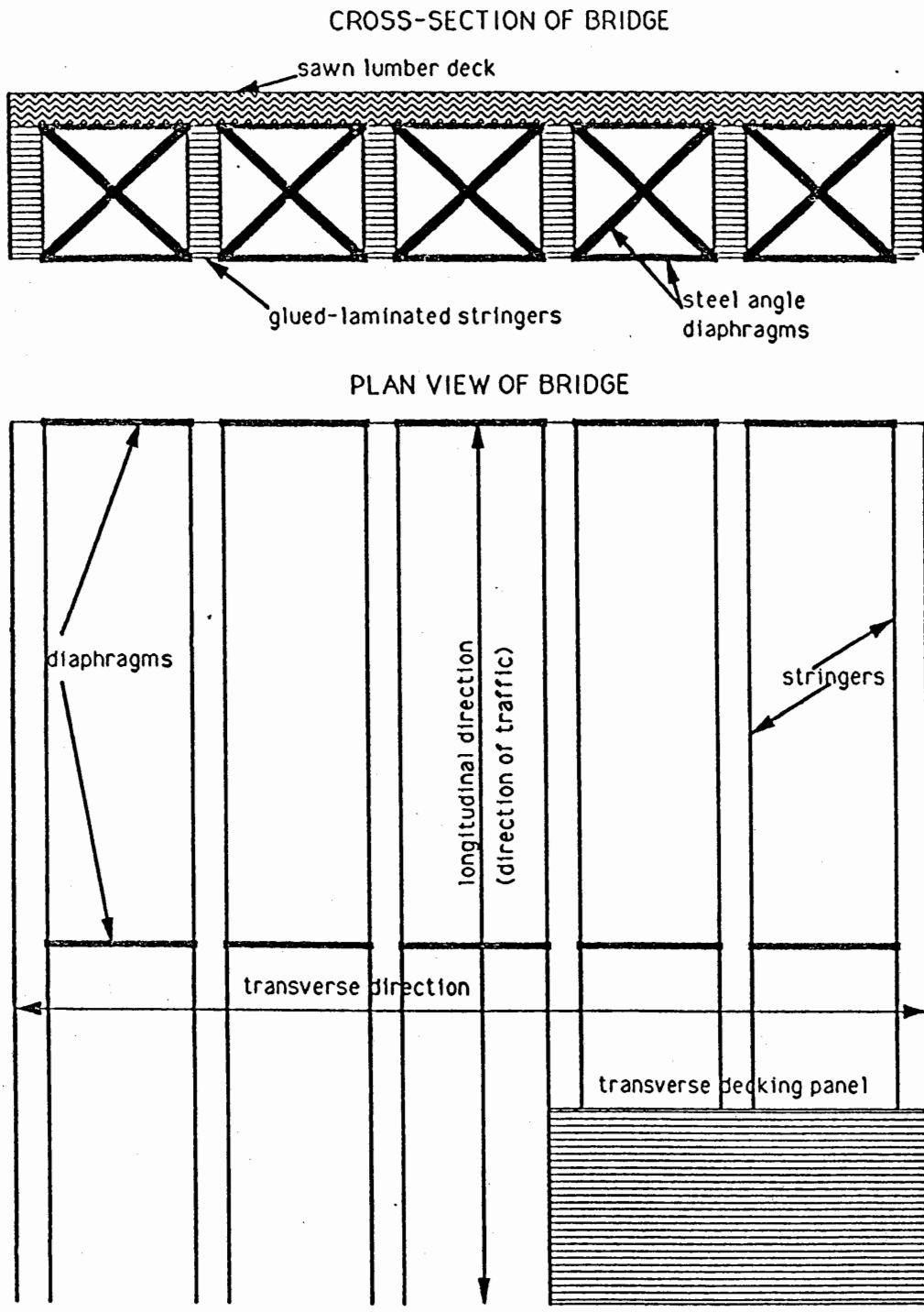


Figure 1. Timber Bridge with Longitudinal Stringers, Transverse Decking, and Diaphragms

investigated. Field testing of a prototype bridge to be built in Canton, CT was originally planned. However, due to numerous delays in construction of the bridge, it was not possible to perform these tests within the scheduled duration of this project. A laboratory testing program was conducted as a substitute for field tests to provide the necessary data on the structural response.

Laboratory tests on bolted and stressed timber deck panels were performed. A small scale model of the bridge was also constructed and tested. A finite element model of the bridge was used to perform the structural analysis. Analyses were performed on the laboratory model and on a typical full-scale bridge (two lane with sixty foot span). The adequacy of current design specifications applicable to this bridge was evaluated. Results from the lab tests and finite element analyses were used to better understand the structural behavior.

Without the construction of an actual bridge, several important considerations for bridge design and construction could not be addressed and, therefore, fall outside the scope of this project. These considerations include corrosion protection, construction procedures, deck to stringer connection, adhesion and cracking of the wearing surface, and actual cost information. If the opportunity to construct the proposed bridge arises in the future, these important considerations would need to be addressed.

2.0 Timber Bridge Deck Study

Laboratory tests were conducted on three different timber panels to determine which design gives the best structural response and which is the most feasible to use as the bridge deck. One way bending tests were performed on laminated beam panels. The panels were simply supported and loaded by a concentrated force at the center as shown in Figure 2. The difference in the panels is the means of connecting the timber laminates. The first panel was bolted together using three mild steel dowels (Figure 2), the second panel was stressed together using two Dywidag tensioning rods, and the third panel was stressed together using two prestressing cables. All three panels were made of Eastern Hemlock.

The bridge deck panels transmit wheel loads to the stringers in both the transverse and longitudinal directions of the bridge (see Figure 1). The panel forces in the bridge's transverse and longitudinal directions will be referred to as the primary and secondary deck forces, respectively. In the laboratory tests, the ability of the different panel designs to carry secondary deck forces is

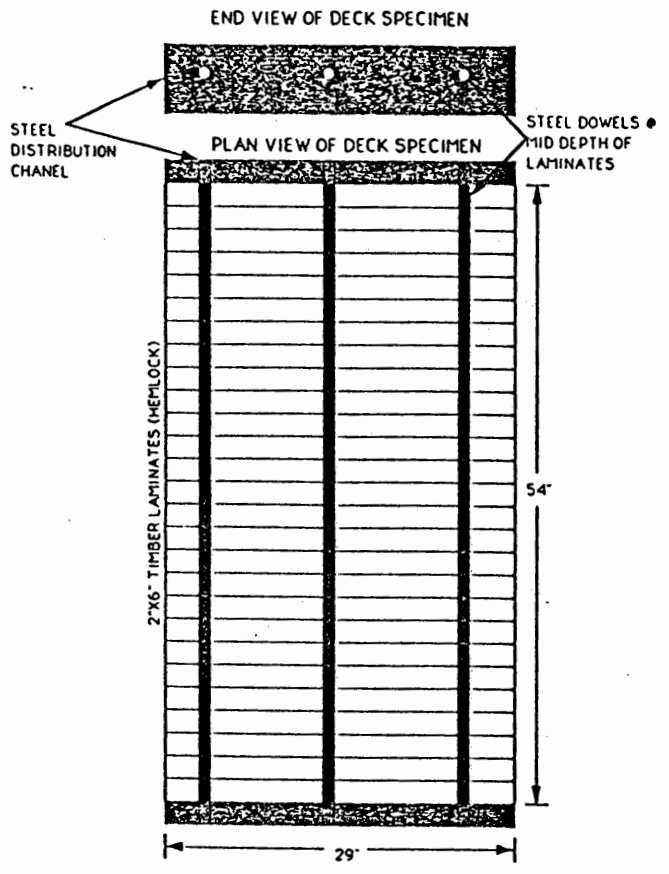
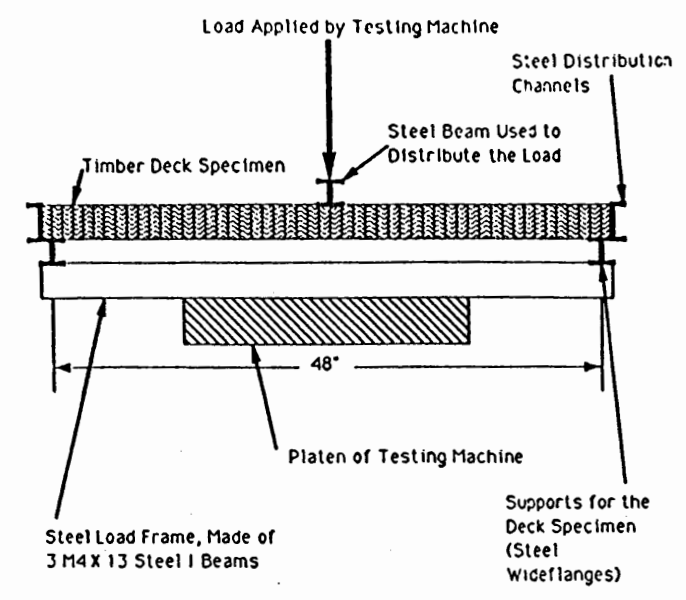


Figure 2. Test Configuration for Timber Panels

tested. It is assumed that the response of the three designs to primary forces is the same.

2.1 Test Results

For a simply supported beam with a concentrated force at midspan, the midspan deflection is given by

$$\delta = \frac{P L^3}{48 EI}$$

where P is the force magnitude, L is the span, and EI is the flexural stiffness of the beam. Two theoretical load-deflection (LD) curves are presented to assist in the evaluation of the test results. The first theoretical LD curve uses the flexural stiffness of three steel dowels and is used in comparison with the first panel (bolted). The second theoretical LD curve corresponds to a solid timber beam using the perpendicular modulus of elasticity for eastern hemlock to compute the flexural stiffness. The two theoretical LD curves are shown in Figure 3. A third LD curve which accounts for combined bending of the wood and steel is also shown, but this response is not significantly different than the second LD curve.

The LD curve for the bolted or dowelled panel is shown in Figure 4a along with the theoretical response for the steel dowels. The stiffness of the dowelled panel is only slightly higher than the stiffness of the steel dowels which means that the timber does not contribute significantly to the stiffness. Figure 4b shows the bending moment carried by the steel dowels at midspan which was determined from strain gauge data. This curve shows that the dowels carry less than half of the total moment for most of the test.

The LD curves for the two stressed panels for different values of prestress force are shown in Figures 5a and 5b for the Dywidag rods and prestressing cables, respectively. The theoretical LD curve for the solid timber beam is shown for comparison. The response of the two stressed panels is similar. As the stressing force is increased, the stiffness of the panels increases but does not reach the theoretical response of the wood. As the load is increased, the LD curves become nonlinear. This is due to crushing of the wood in the region associated with compressive bending stresses. The combined compressive stresses due to prestress force and bending eventually exceed the crushing strength of the wood as the load is increased.

According to the new design guide for stressed decks [1], one criteria for determining the magnitude of the tensioning force is that there is no net tension in the deck

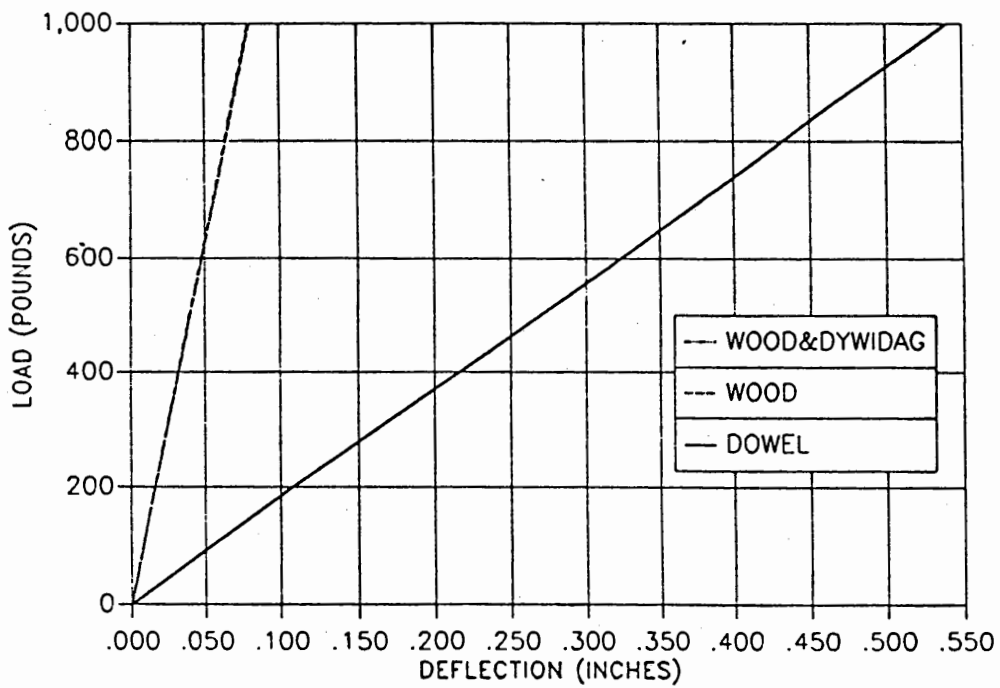
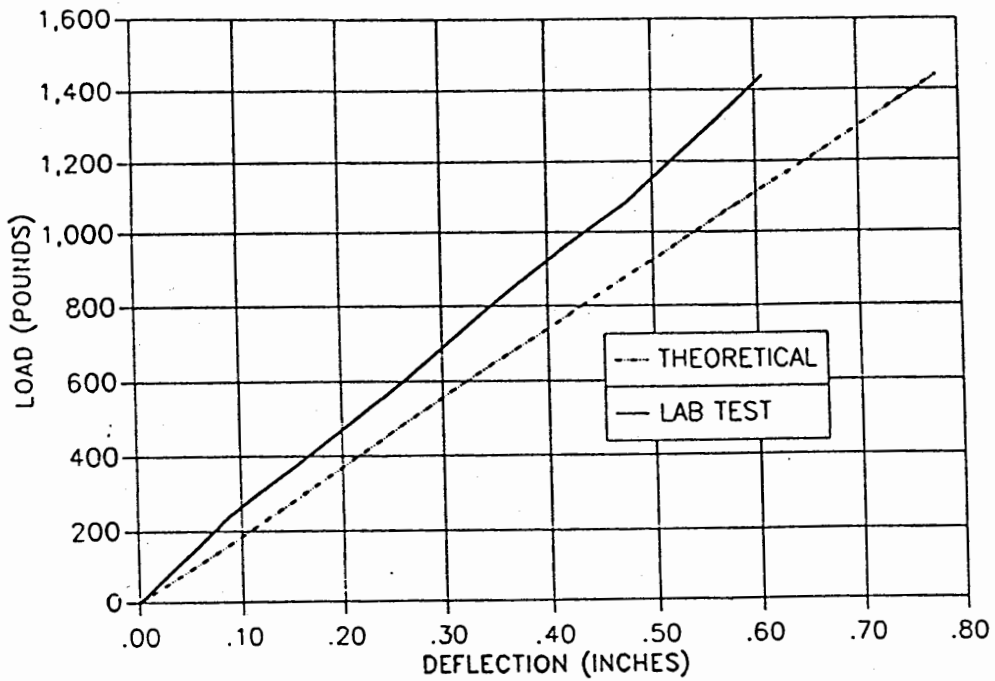
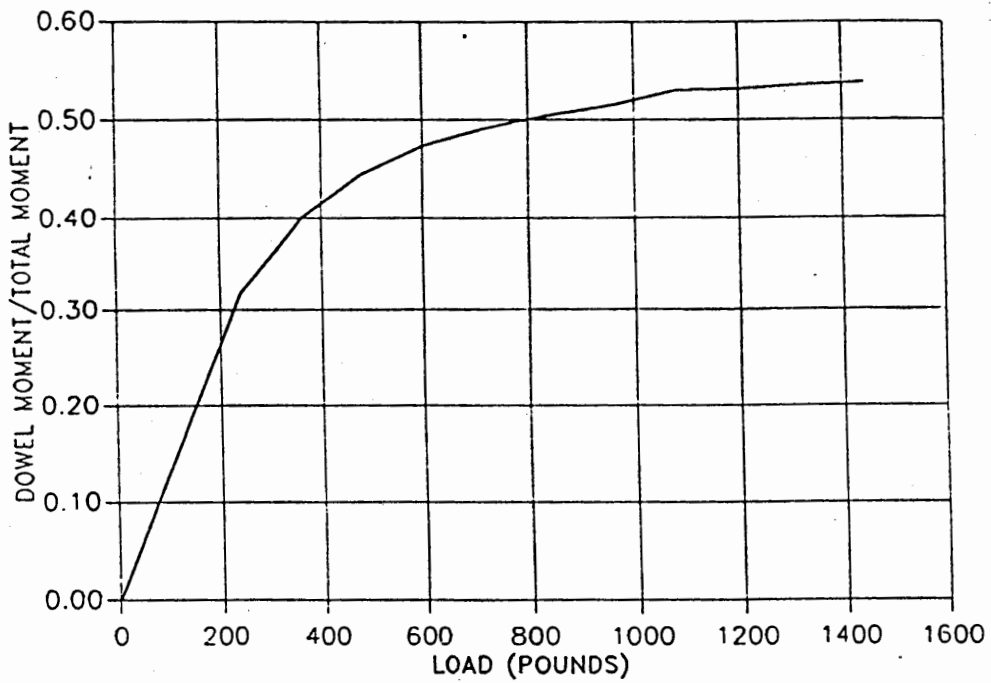


Figure 3. Theoretical Load-Deflection Curves for Steel Dowels, Solid Wood Section, and Solid Wood Section with Dowels

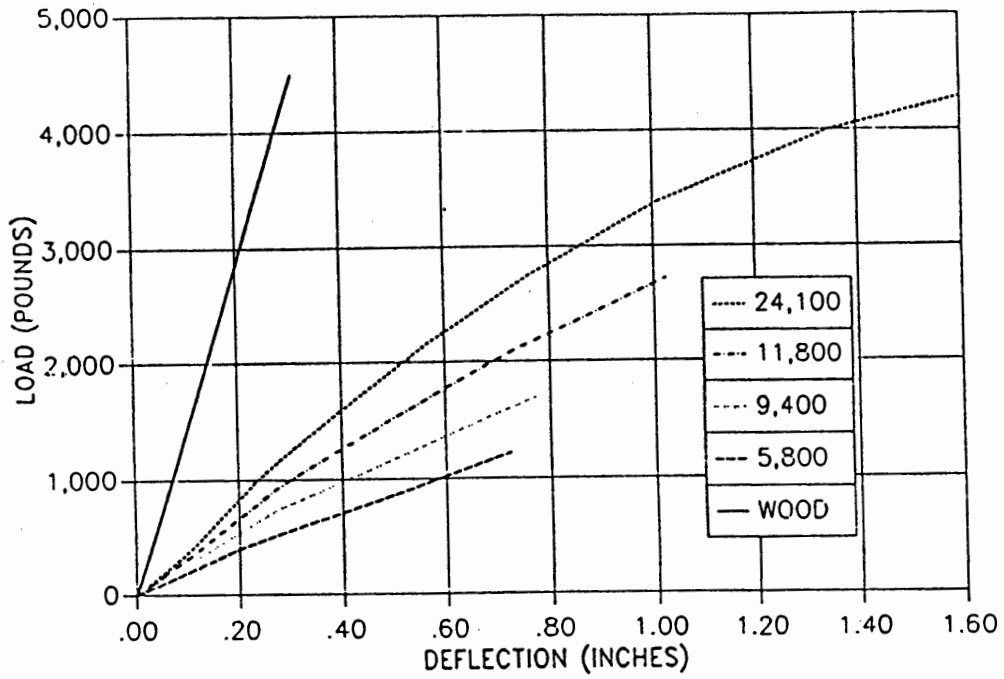


(a)

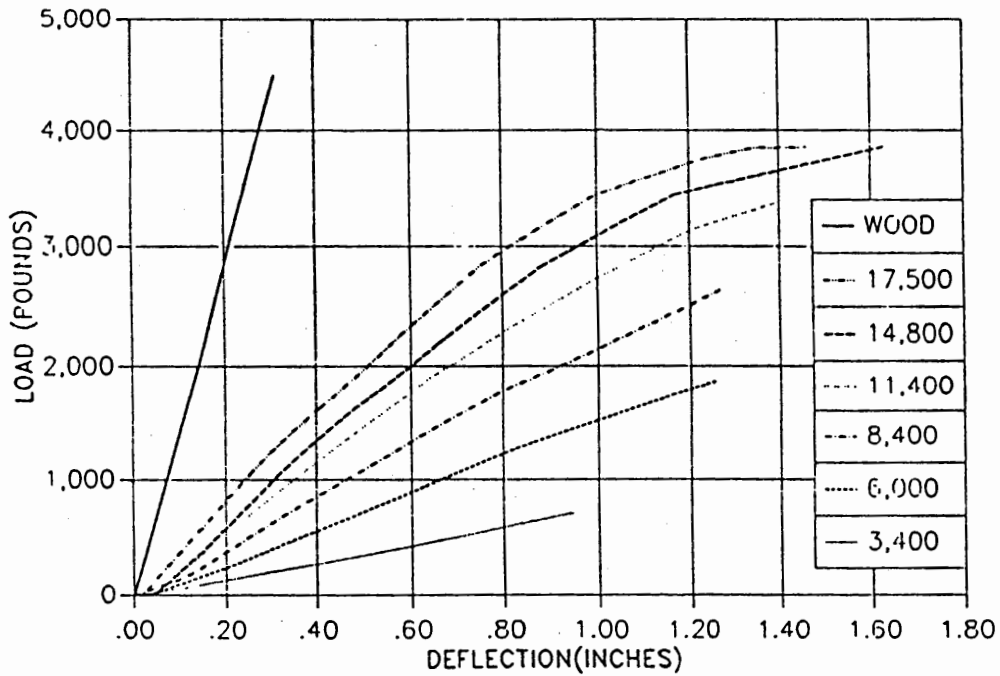


(b)

Figure 4. Lab Test of Bolted Deck Panel, (a) Load-Deflection Curve, (b) Bending Moment Carried by Steel Dowels



(a)



(b)

Figure 5. Load-Deflection Curve for Stressed Deck Panels, (a) Dywidag Rods, (b) Prestressing Cable

panel under the combined compression and bending stresses since the laminated panel can not support tension. The load at which interlaminar tension begins was calculated for the panels tested, but no significant change in the LD curves was found to occur at these loads.

The stiffness of the three panels normalized by the theoretical stiffness for a solid wood section is shown in Figure 6 as a function of stressing force. The curves for the panels using the Dywidag rods and prestressing cable are fairly similar. For the stressed panels with realistic tensioning force and for the dowelled panel, the panel stiffnesses are only about 20% of the theoretical solid wood stiffness.

2.2 Feasibility of Deck Construction

In addition to measuring the load-deflection response of the three panels, the feasibility of each panel design for an actual bridge deck was evaluated. The bridge deck considered is 60 feet long and 27.5 feet wide and was designed according to AASHTO requirements (see Appendix).

The first consideration is the amount of steel required and number of holes to be drilled through the timber laminates. According to the design, the dowelled deck requires one dowel every 11 inches across the width. This translates into 10,824 pounds of steel and 10,800 holes. For the stressed decks, a stressing rod or cable is used every 66 inches across the width. This results in 1,084 pounds of Dywidag rod or 799 pounds of prestressing cable and 2,160 holes. The dowelled deck requires about 10 times as much steel and 5 times as many holes as the stressed decks. It is expected that a dowelled deck would cost significantly more than either of the stressed decks.

The details of connecting a bolted or dowelled deck have not been fully established. Bolted deck panels could easily be assembled, but these would have to be further connected in the field to form the bridge deck. For the stressed decks, the Dywidag rods or prestressing cable would run continuously along the length of the bridge. Loss of tensioning force due to creep is a concern. Access to the ends of the tensioning rods or cables would be necessary to allow for retensioning.

The prestressing cables appear to have several advantages over the Dywidag rods. First, the cables have a higher strength and, therefore, a lower stiffness than the rods. It has been shown that lower stiffness in the tensioning components results in lower losses of tensioning force due to creep [3]. The stiffness of the cables is about half of the stiffness of the rods [4]. Second, the cables

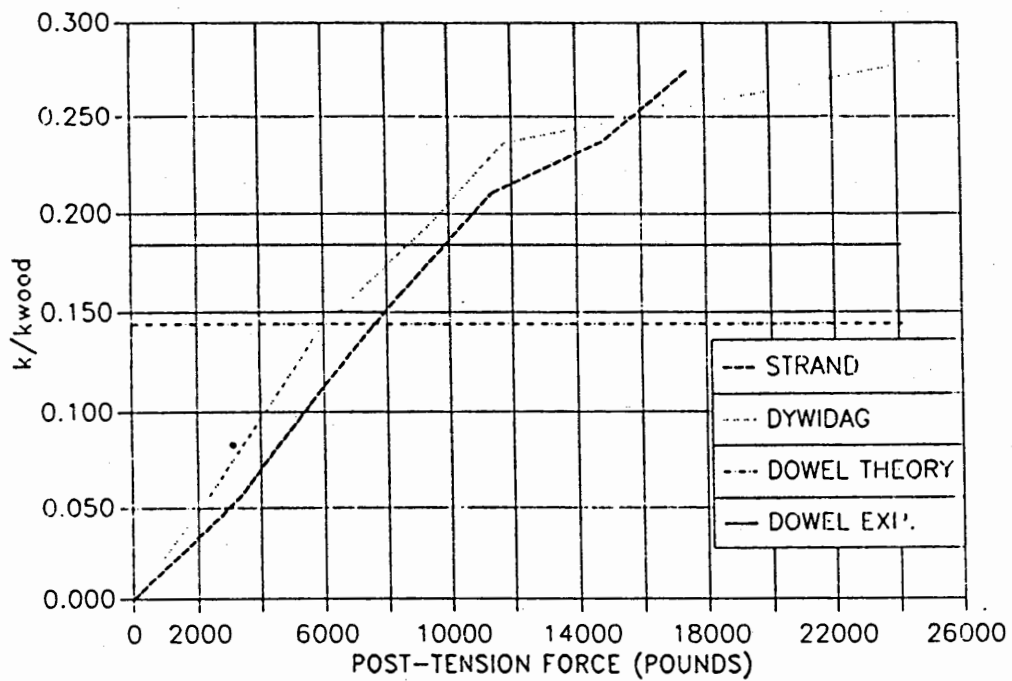


Figure 6. Normalized Stiffness of Deck Panels

are more flexible which simplifies construction. Finally, prestressing cables are more available than Dywidag rods and are less expensive. Damage to the cables by the anchor chucks and difficulty in restressing the cables are the primary disadvantages [2].

3.0 Bridge Model Tests

Laboratory tests on a 1/12 scale model of the proposed bridge were performed to evaluate the structural response of a timber bridge with timber stringers, steel diaphragms, and a timber deck. The test results are compared to the predictions from a finite element model which is described in Chapter 4. The model and testing configuration are shown in Figure 7. The model was simply supported and loaded with a concentrated force at the center. The deflection of the model across the midspan was measured. The model consisted of 1"x4" douglas fur stringers, 3/4" thick pine deck, and diaphragms made from 1/2"x1/2"x1/8" steel angles.

The primary purpose of the tests was to see how the diaphragms affect the structural response. The effect of diaphragms is not included in the AASHTO design code for timber bridges. The response of the model with and without diaphragms, and with stiffened diaphragms was measured.

3.1 Test Results

A test was first performed at several load levels to establish the linearity of the structural response. Figure 8 shows the load versus center deflection for the bridge model with diaphragms, which confirms that the response was linear. The bridge model was then tested without diaphragms. The deflection across the midspan for this test is shown in Figure 9 along with predictions from the finite element model with and without diaphragms. The test was repeated several times. The similarity of the curves shows the reproducibility of the tests. The agreement of the lab results with the finite element model without diaphragms is good. Comparing the two finite element predictions, it is seen that the diaphragms should significantly stiffen the bridge in the transverse direction.

The model was next tested with the diaphragms but without the deck. It should be noted that there was no significant difference between the finite element results with and without the deck when the model has diaphragms. This means that the diaphragms contribute much more to the transverse stiffness than the deck. The results of the lab test are shown in Figure 10. It can be seen that the test results do not agree with the finite element model with diaphragms. It is only a coincidence that the lab data

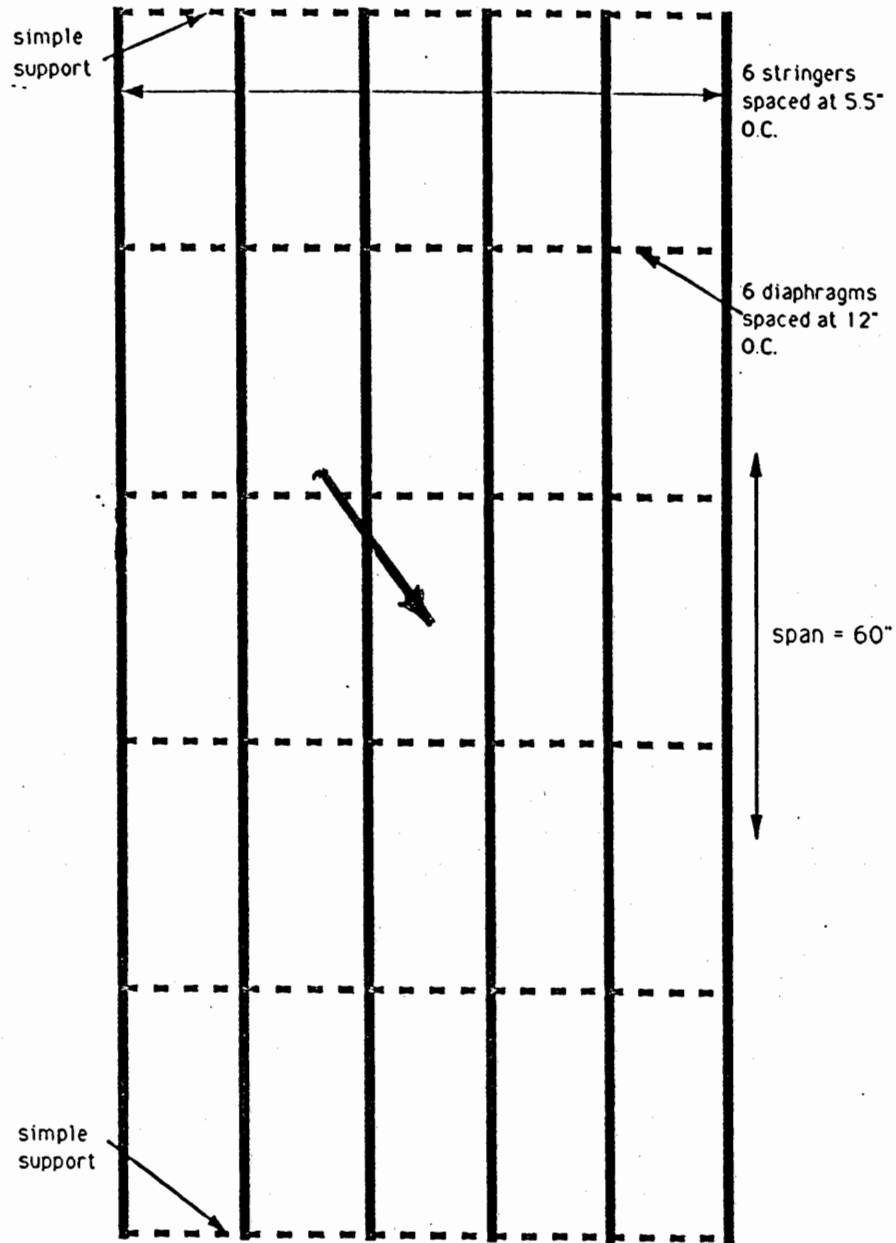


Figure 7. Testing Configuration used for Small Scale Bridge Model

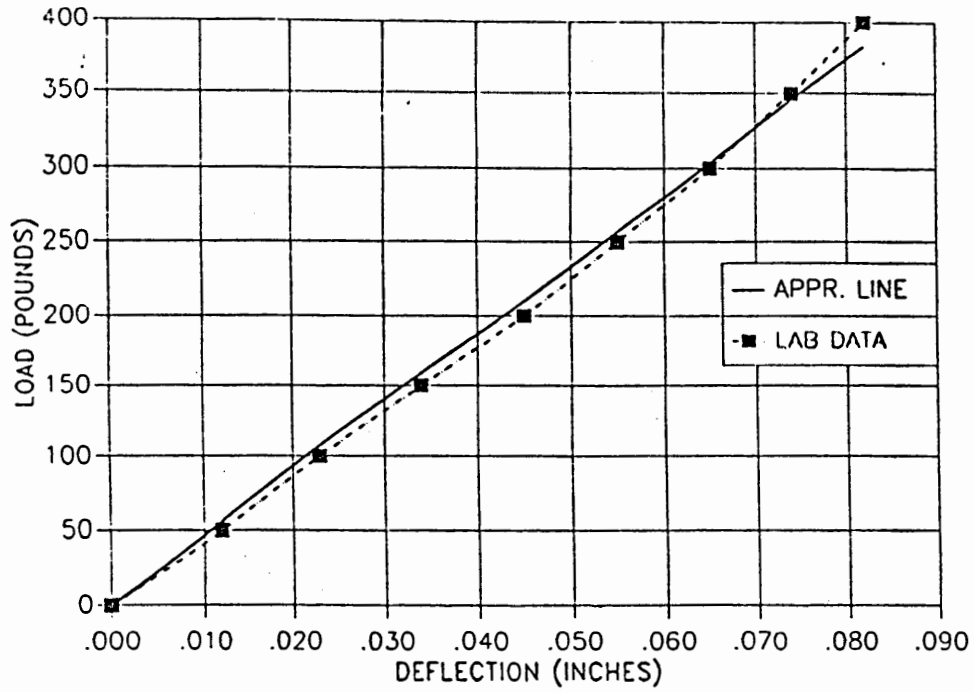


Figure 8. Load-Deflection Curve for Bridge Model

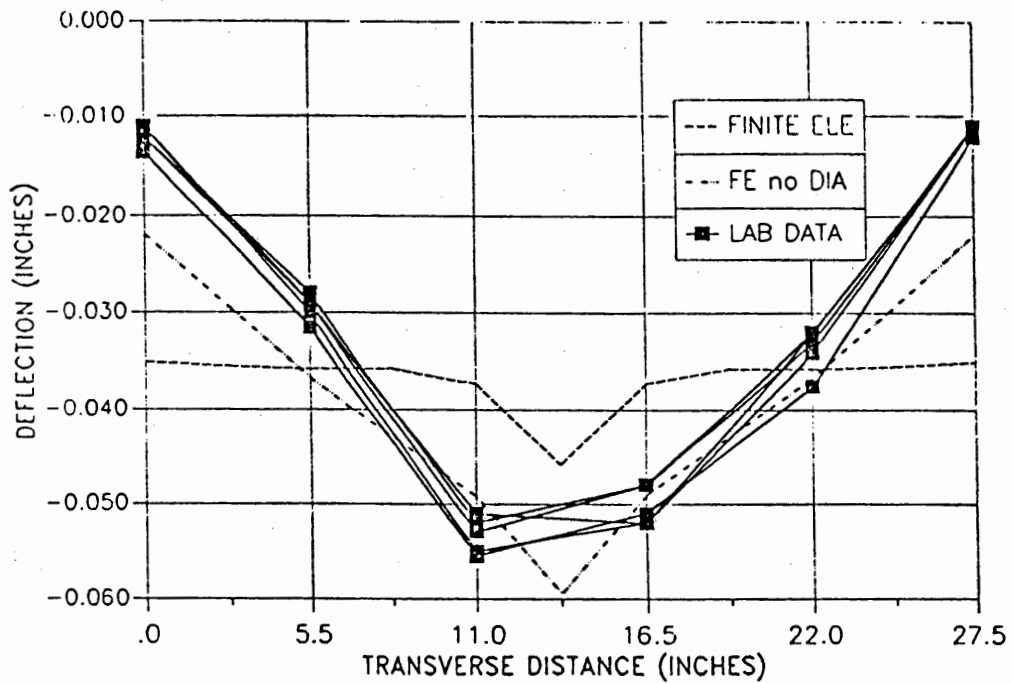


Figure 9. Transverse Deflection of Bridge Model at Midspan without Diaphragms

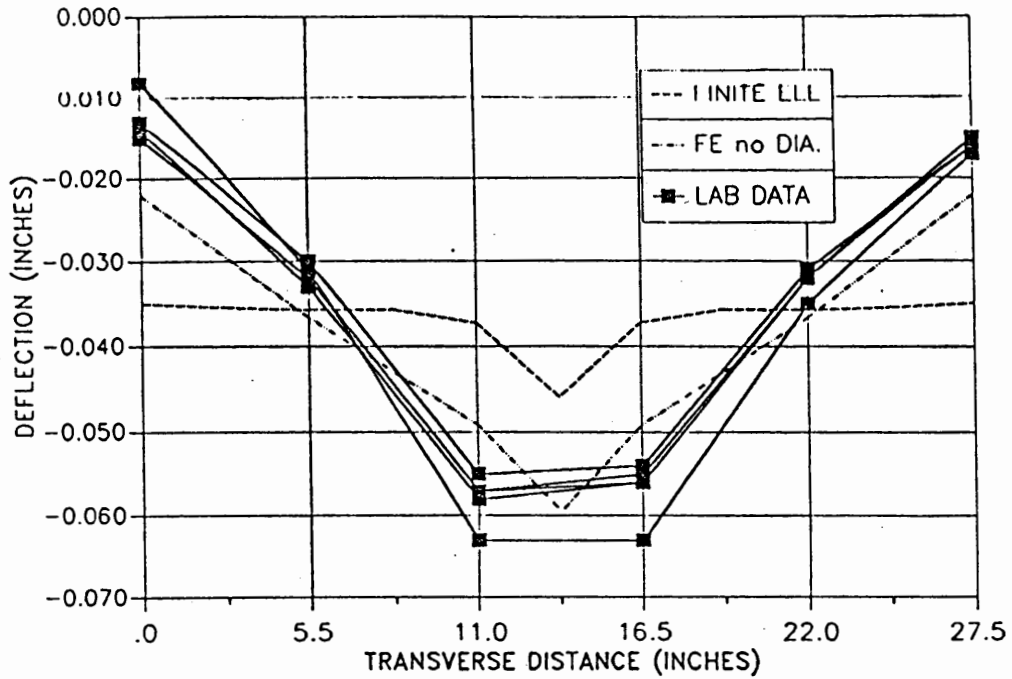


Figure 10. Transverse Deflection of Bridge Model at Midspan with Diaphragms

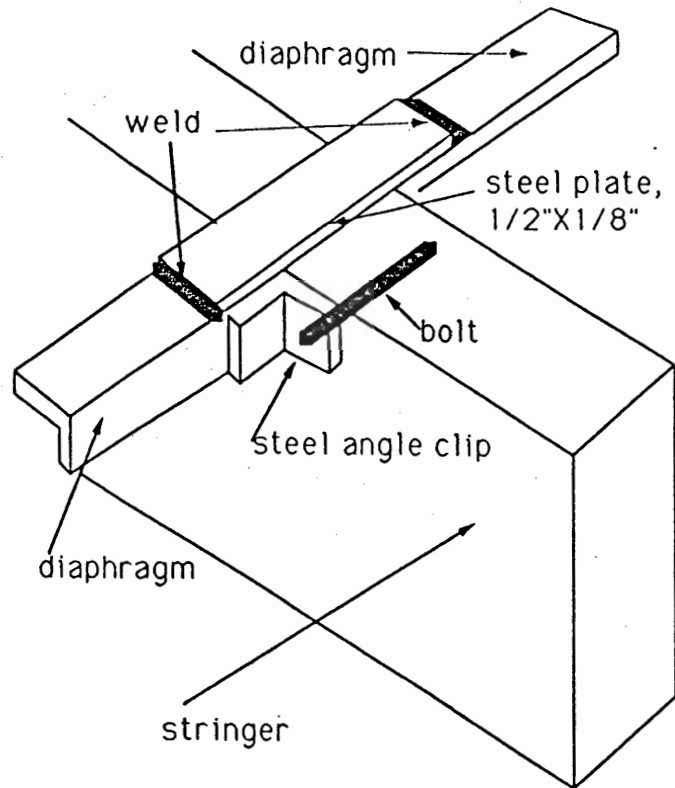


Figure 11. Diaphragm to Stringer Connection

appears to agree with the finite element model without diaphragms.

The reason for the large discrepancy between the predicted and measured response of the model with diaphragms was attributed to flexibility in the connections between the diaphragms and the stringers. The connections consisted of steel angle clips and through bolts as shown in Figure 11. A steel plate was welded between adjacent diaphragms, as shown in Figure 11, in an attempt to stiffen the diaphragm connections. The lab results for the model with welded and unwelded diaphragms is shown in Figure 12. A dramatic increase in transverse stiffness was achieved by welding the diaphragm connections. The response of the welded system is much closer to the finite element model which assumes infinitely rigid connections.

4.0 Analysis of Timber Bridge Behavior

A finite element model of the proposed timber bridge was developed to better understand the structural behavior of the bridge. The model was used to predict bridge deflection and deck and stringer forces which were compared to those given by existing design codes. An important consideration in developing the model was whether the bridge deck acts compositely with the stringers. For the longitudinal direction, the contribution to composite behavior from the deck is small because its small thickness and the low modulus of elasticity of the deck in this direction. For the transverse direction, a separate model was constructed to evaluate the importance of composite behavior. It was found that the difference in maximum deflection for composite and noncomposite behavior was less than 8% for both the longitudinal and transverse directions. Since the means of connecting the deck to the stringers in actual construction does not insure composite behavior, and since the importance of composite behavior is small, the effect of composite behavior was neglected in developing the finite element model.

A two-dimensional finite element model was developed to represent the three-dimensional bridge as shown in Figure 13. To achieve this, a one-dimensional "diaphragm element" was derived to represent the actual two-dimensional diaphragms [4]. In order to test the validity of the diaphragm element and to assess the significance of composite behavior, several finite element analyses were performed on the bridge cross-section as shown in Figure 14. The two-dimensional models in Figures 14a and 14b are the actual bridge cross-section for composite and noncomposite behavior, respectively. The models are supported on springs with stiffness equal to the stiffness of the stringers at midspan. A concentrated force

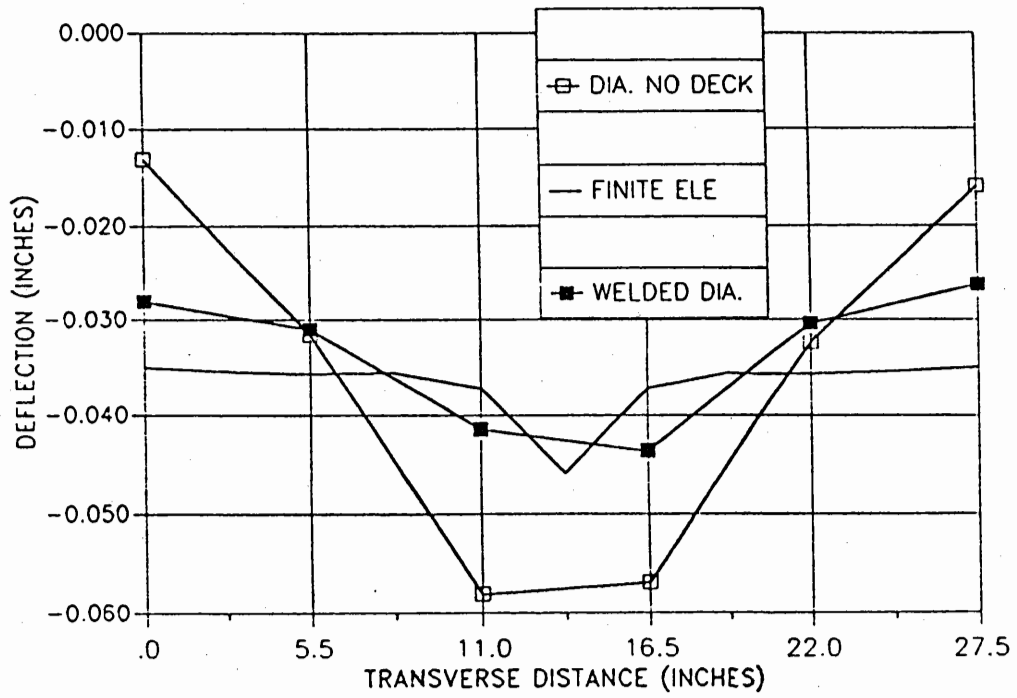
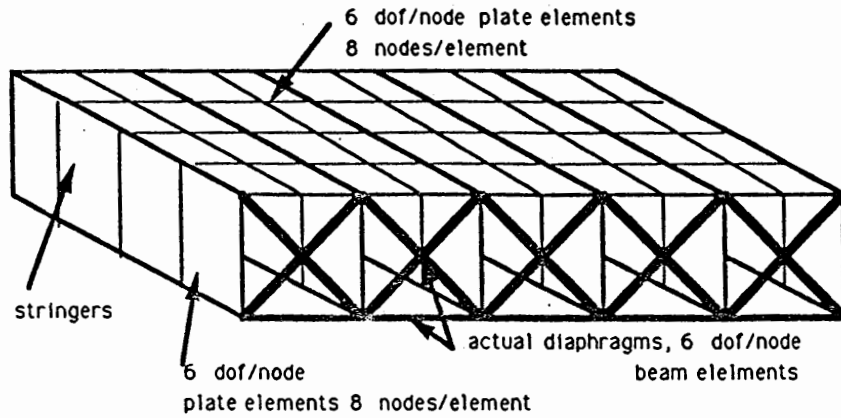
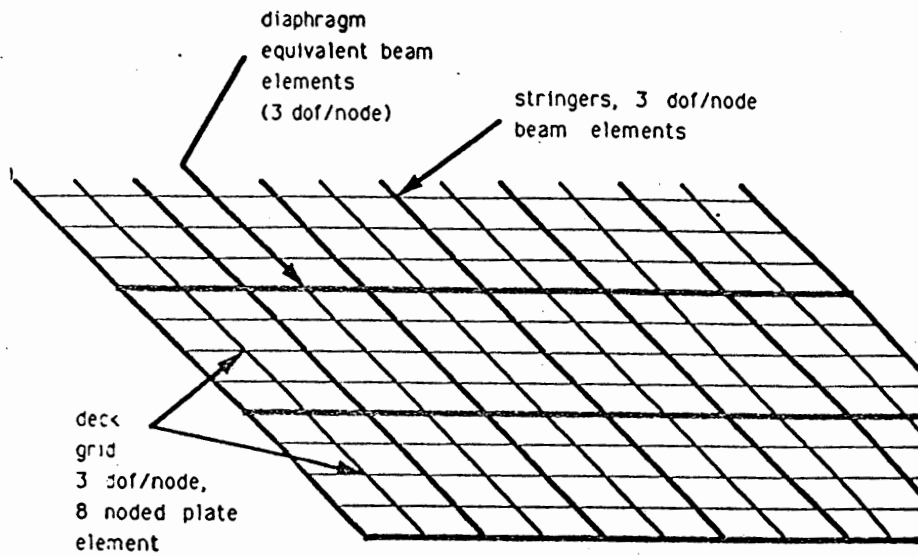


Figure 12. Transverse Deflection of Bridge Model at Midspan with Welded Diaphragms and No Deck

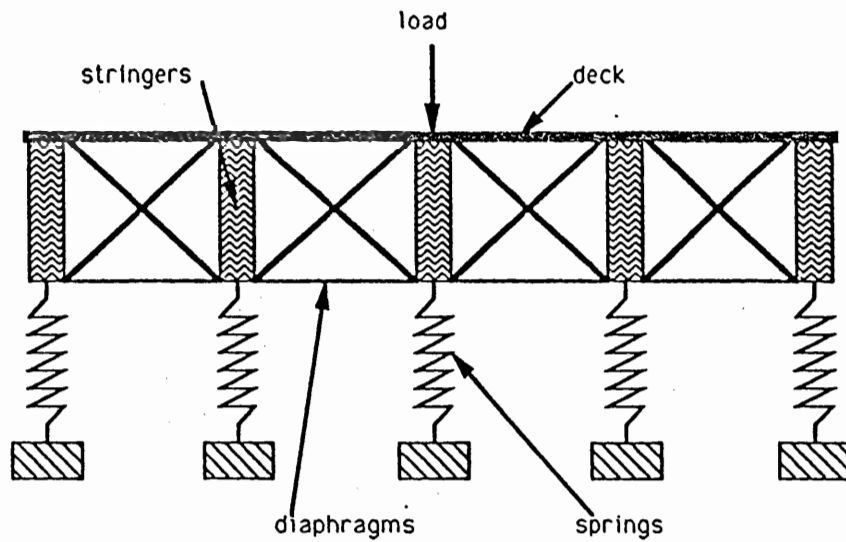


(a)

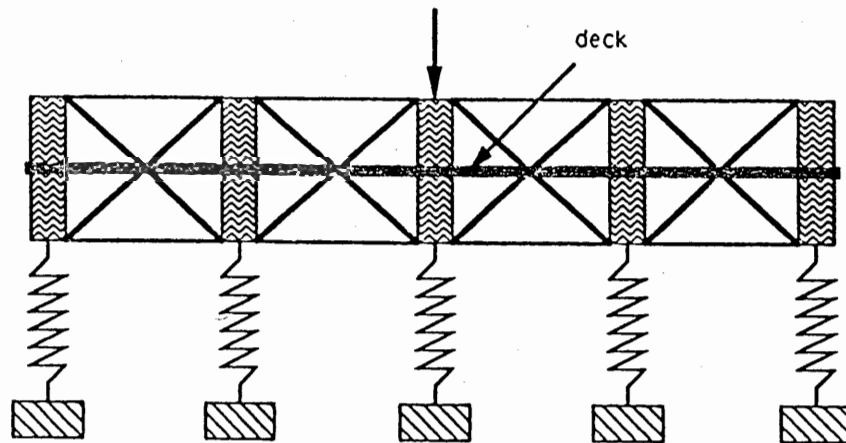


(b)

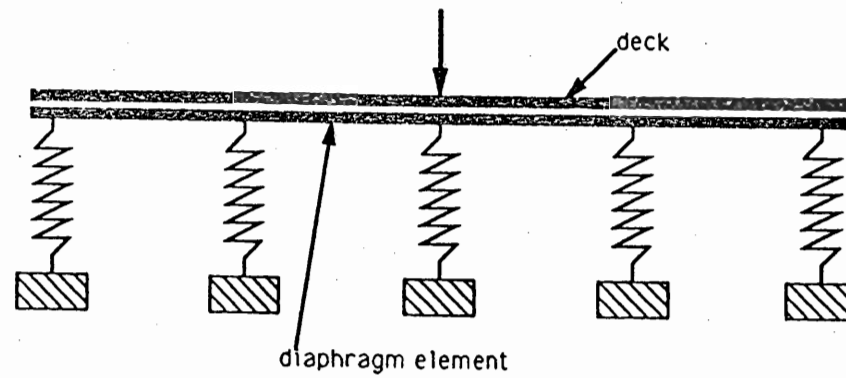
Figure 13. Timber Bridge and the Finite Element Model, (a) Three-Dimensional Bridge, (b) Two-Dimensional Finite Element Model



(a) Two-Dimensional Composite Model



(b) Two-Dimensional Noncomposite Model



(c) One-Dimensional Noncomposite Model

Figure 14. Finite Element Models of Transverse Section

is applied at the center. The model shown in Figure 14c uses one-dimensional diaphragm elements to represent the actual diaphragms. The response of the three models is shown in Figure 15. It can be seen that the model using diaphragm elements is identical to the two-dimensional noncomposite model, and that the difference between the composite and noncomposite behavior is small.

4.1 Analysis of Deck Forces

In order to design the timber bridge deck, the primary and secondary forces in the deck, corresponding to the transverse and longitudinal bridge directions respectively, must be evaluated. AASHTO design specifications for deck forces in a glue-laminated timber deck are available which are based on research performed at the Forest Products Laboratory (FPL) [5,6,7]. These design specifications can be applied to other types of transverse decking as proposed here and, therefore, the adequacy of these design specifications in predicting deck forces was evaluated.

The deck forces given by the FPL work are based on a simplified geometry of the actual bridge. Namely, FPL considers deck forces due to a wheel load on a simply supported orthotropic plate of infinite length. The simple supports represent two adjacent stringers and, therefore, they do not account for continuity of the deck. Also, FPL assumes that the plate is "thin", which implies that the span to thickness ratio of the deck is greater than 20:1. For the proposed bridge deck and for other reasonable deck designs, the bridge deck is considered "thick", having a span to thickness ratio of only 6:1. As noted by Taylor [8], the use of thick plate theory for the bridge deck is more appropriate. In this study, the results of the finite element analysis are compared to FPL results to evaluate the adequacy of the assumed simplified geometry and thin plate assumption in predicting the deck forces.

The deflection across midspan due to a 16 kip wheel load at the center of the bridge as predicted by FPL and the finite element (FE) model is shown in Figure 16. The FPL result is larger than the thin plate FE result since deck continuity is neglected. The thick plate FE result is significantly greater than the thin plate FE result because thick plate theory allows for shear deformation which increases the flexibility of the plate. It is only coincidental that the FPL result and thick plate FE result agree relatively closely.

The primary moment and shear for the deck are shown in Figure 17. The FPL result for primary moment agrees well with the thin plate FE results. However, the primary

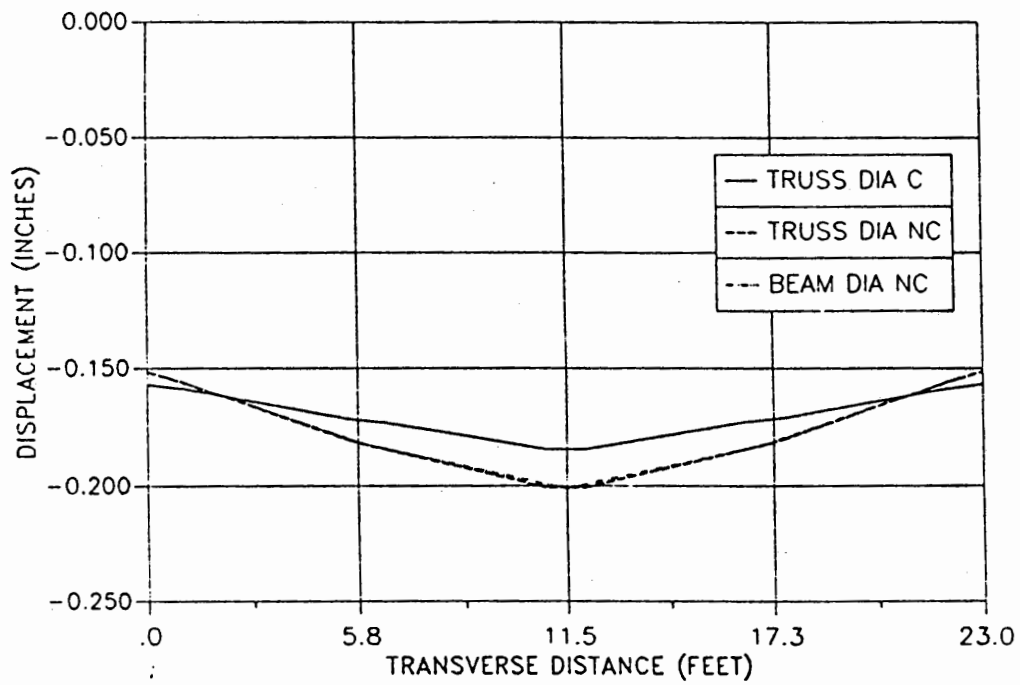


Figure 15. Transverse Deflection of the Three Models

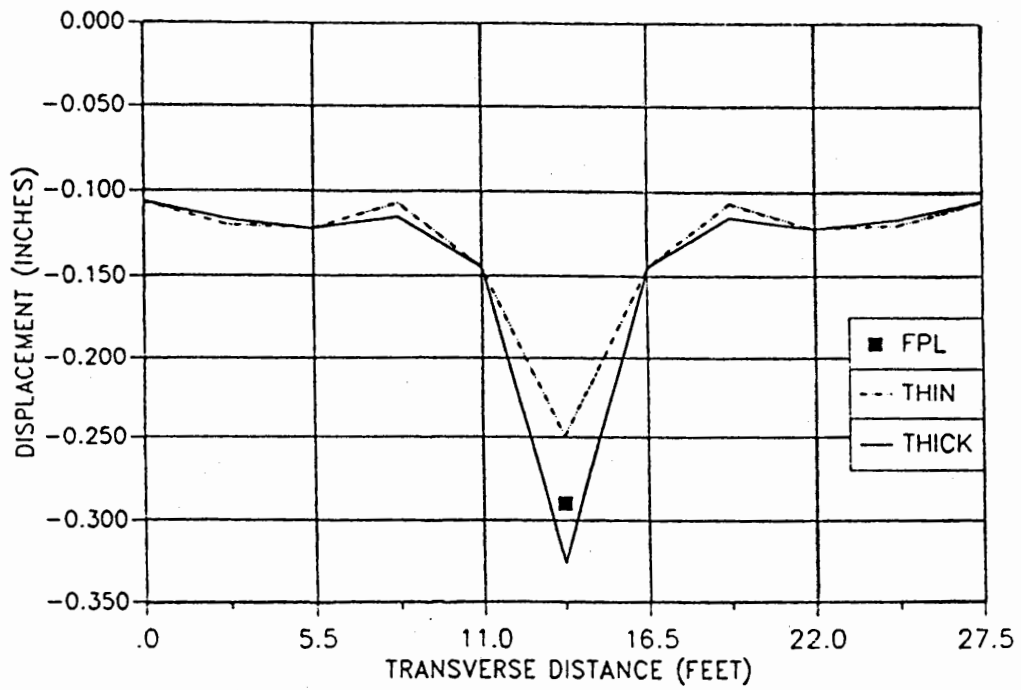
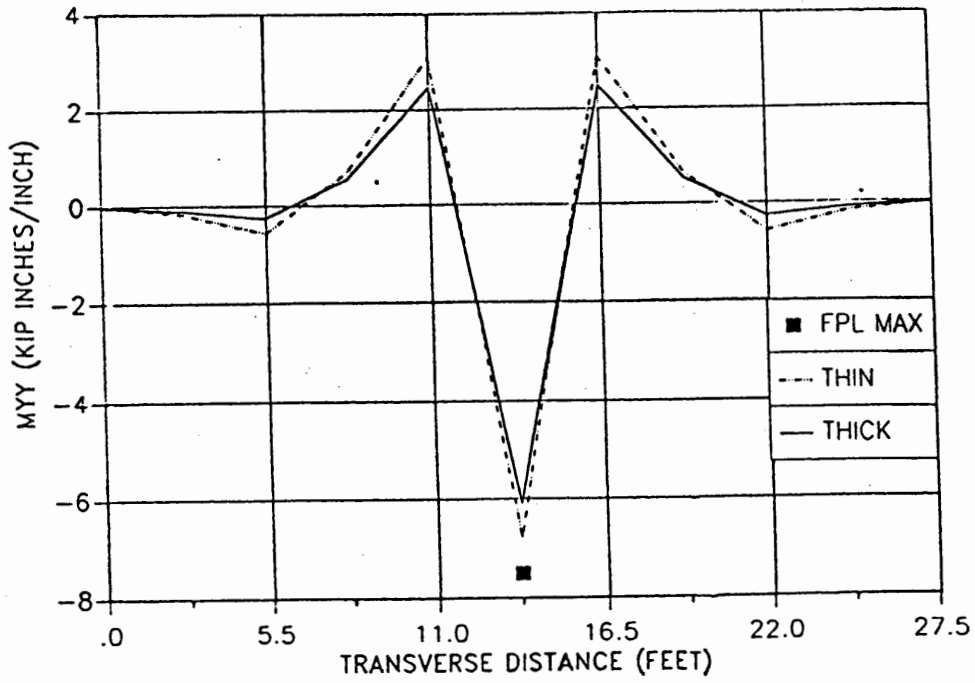
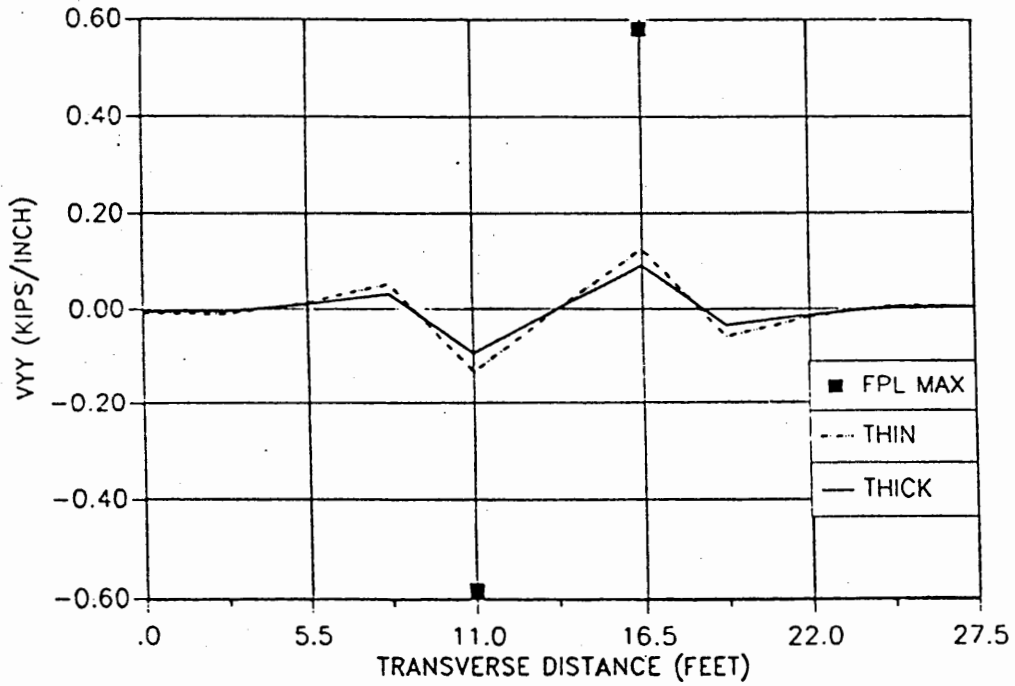


Figure 16. Transverse Deflection of Bridge



(a)



(b)

Figure 17. Primary Deck Forces, (a) Primary Moment, (b) Primary Shear

shear is much larger than the thin plate FE prediction. The difference between the thin and thick plate FE results for primary moment and shear is small. The secondary moment and shear for the deck are shown in Figure 18. For both quantities, the FPL result is significantly higher than both FE results. The difference between thin and thick plate FE results for secondary forces is also significant.

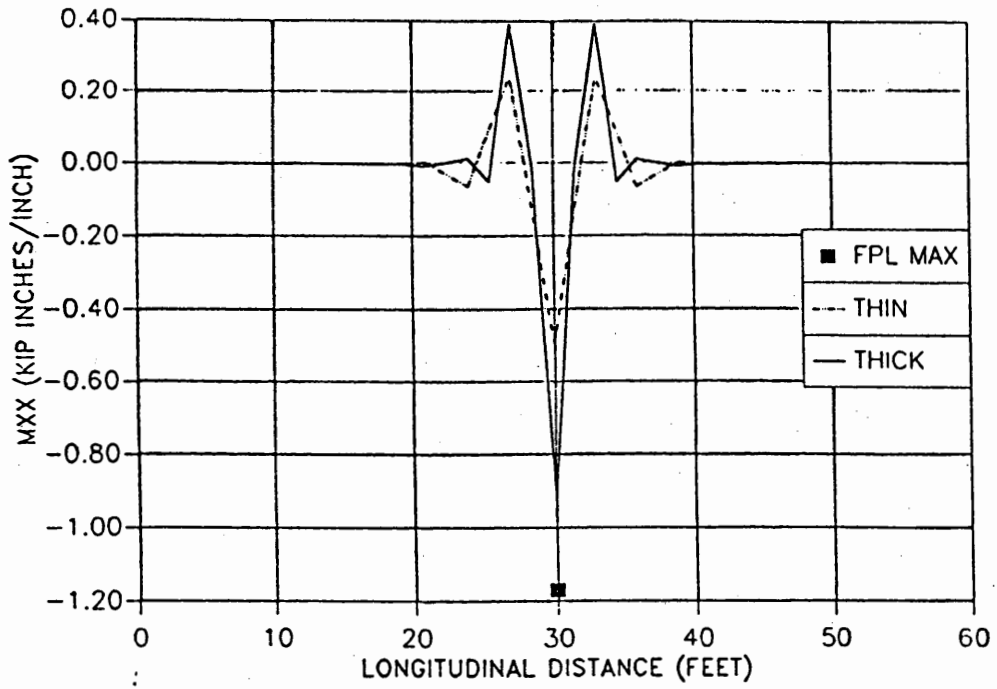
For the above calculations, the modulus of elasticity of the wood perpendicular to grain was used for the bridge deck in the longitudinal bridge direction. As was noted in Chapter 2, this stiffness is not achieved when the deck is laminated as proposed here. The FE calculations were evaluated again using 20% of this stiffness. This value was considered a reasonable average from the results obtained in the various laboratory tests. Figure 19 shows the midspan deflection for full and 20% stiffness. As expected, the local deformation between the stringers increases quite dramatically; however, the global deflections are fairly close. Figures 20 and 21 show the primary and secondary forces in the deck, respectively. The reduction in deck stiffness increases the primary forces and decreases the secondary forces by a significant amount.

4.2 Analysis of Stringer Forces

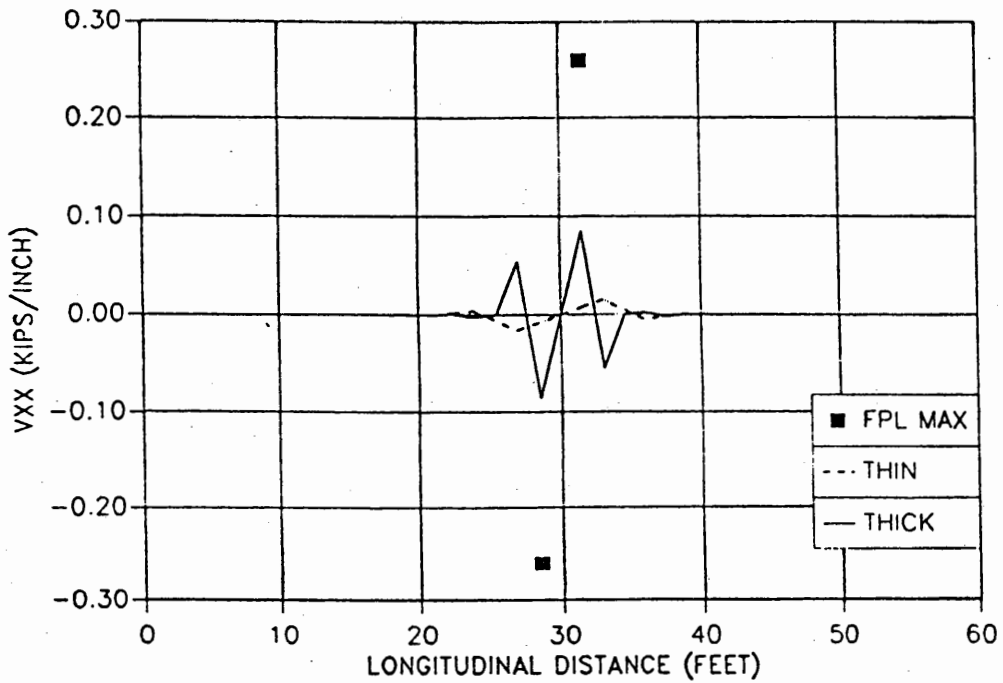
The finite element model was also used to analyze moment and shear in the stringers due to a HS 20-44 truck load. The results of the analysis are compared to the AASHTO design method. The effect of diaphragms on the structural behavior of the bridge is also considered. It was seen in Chapter 3 that the diaphragms have a strong effect on the transverse stiffness of the bridge. The effect of diaphragms on the structural behavior of the bridge is not included in current design specifications.

The truck loads were applied to the FE model to produce the maximum stringer moment and shears according to AASHTO specifications. For maximum moment, the distance from the resultant truck loading to the bridge centerline shall equal the distance from middle axle to centerline as shown in Figure 22. For maximum shear, the position of the last wheel load from the support is the lesser of three times the stringer depth or one quarter of the bridge span. The placement of the truck loads on the FE model to produce maximum stringer moments is shown in Figure 22.

The moment and shear diagrams from the FE model for the stringer directly under the wheel load with two trucks on the bridge are shown in Figure 23 along with the AASHTO values. It is seen that the AASHTO values agree well with the maximum



(a)



(b)

Figure 18. Secondary Deck Forces, (a) Secondary Moment, (b) Secondary Shear

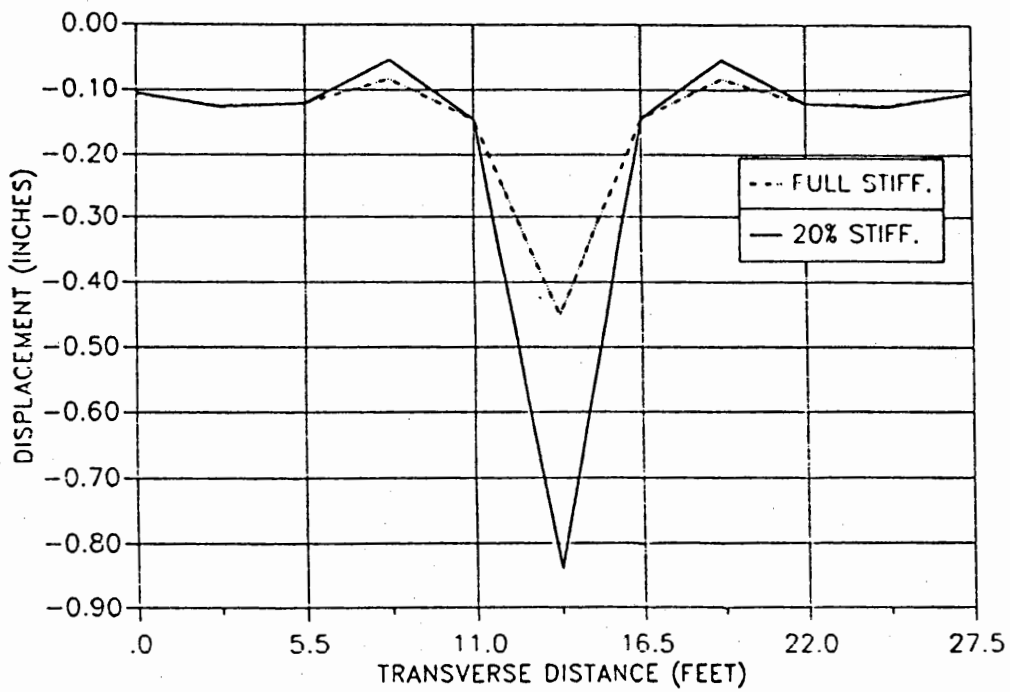
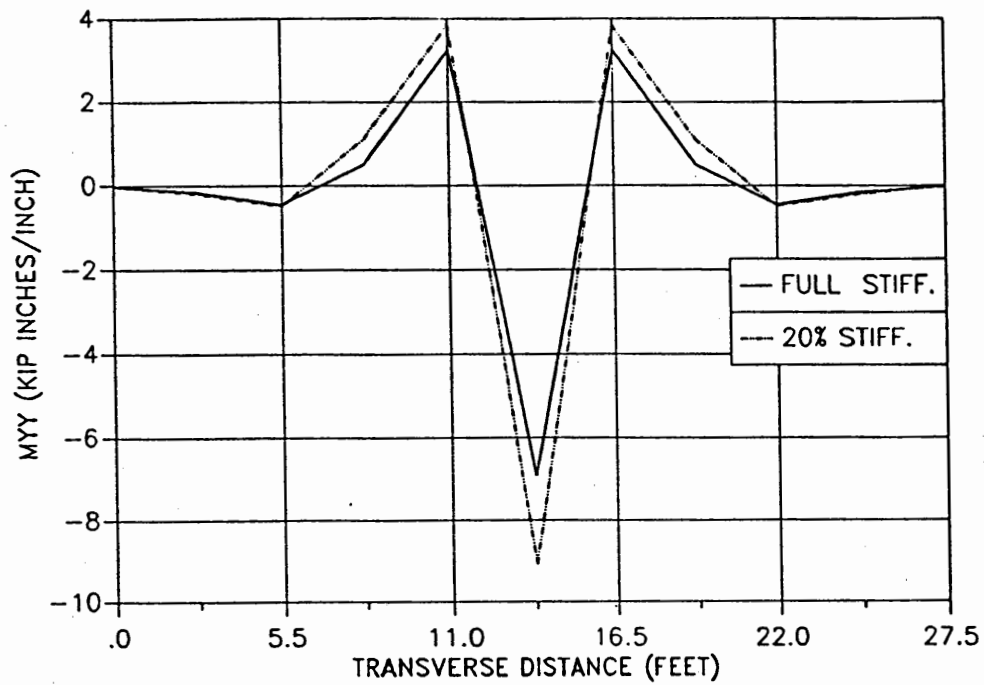
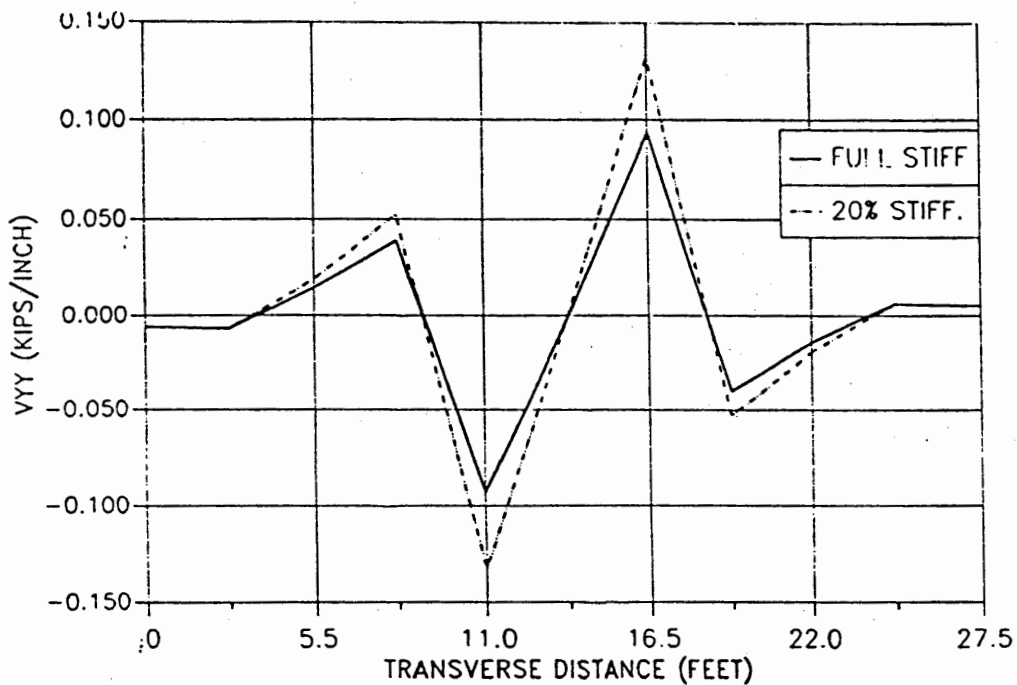


Figure 19. Transverse Deflection of Bridge with Reduced Stiffness

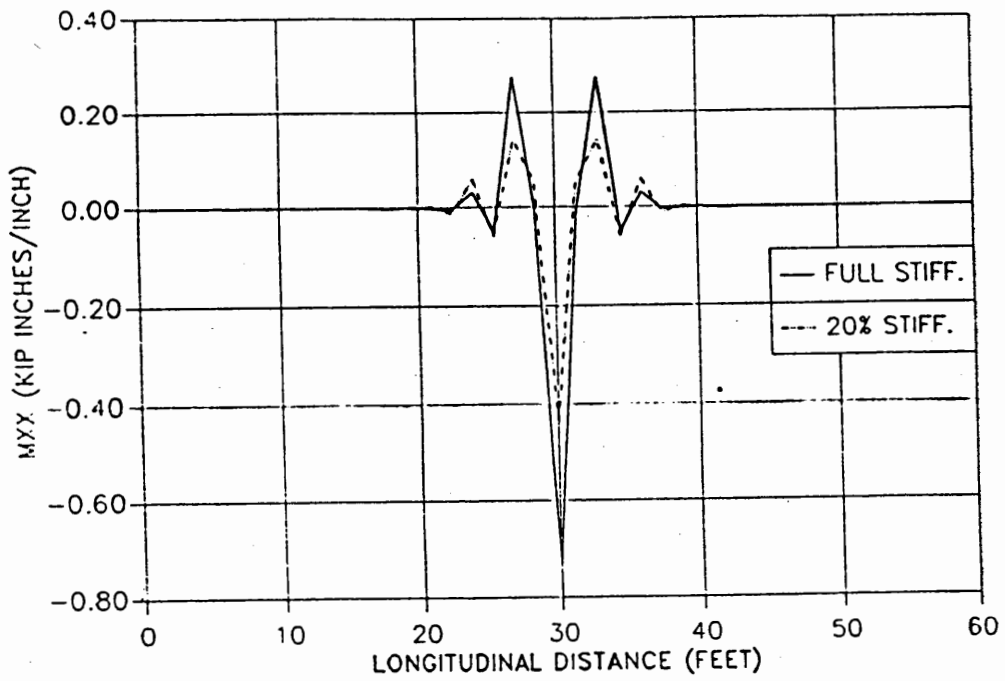


(a)

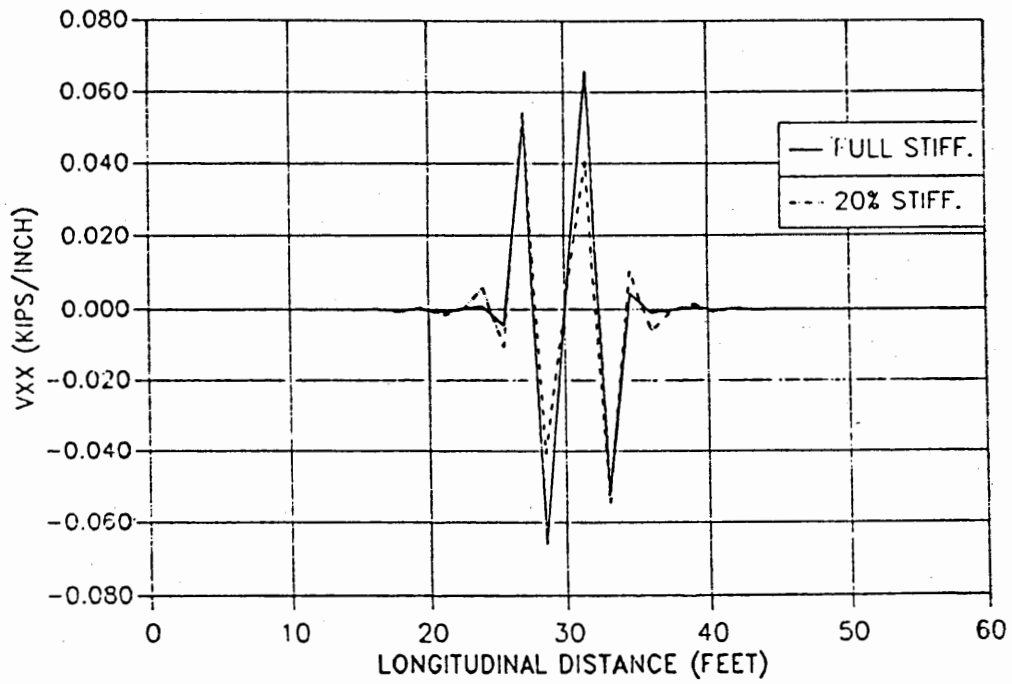


(b)

Figure 20. Primary Deck Forces with Reduced Stiffness, (a) Primary Moment, (b) Primary Shear

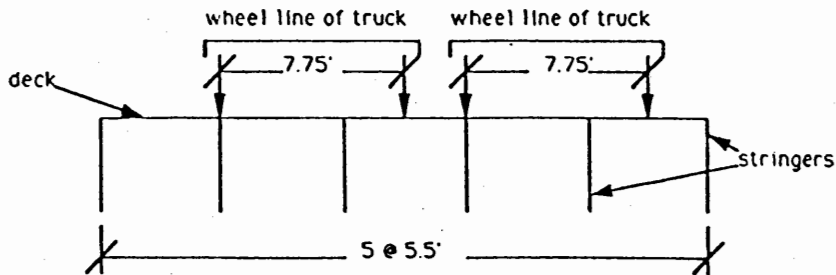
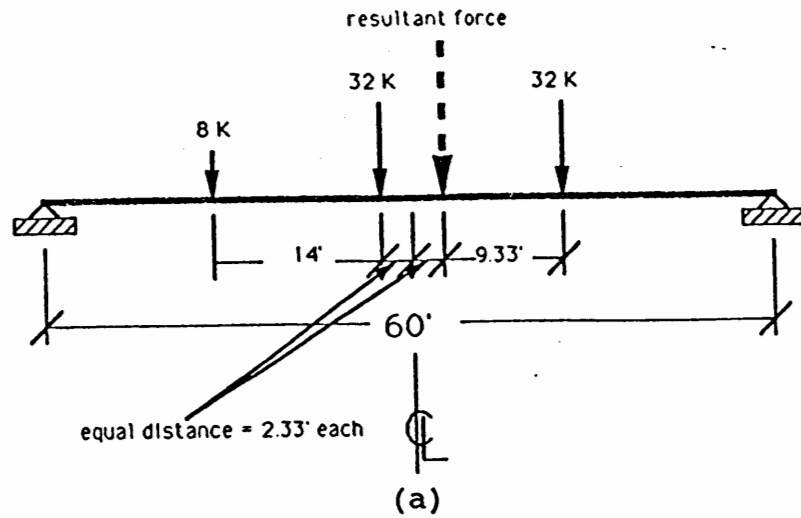


(a)

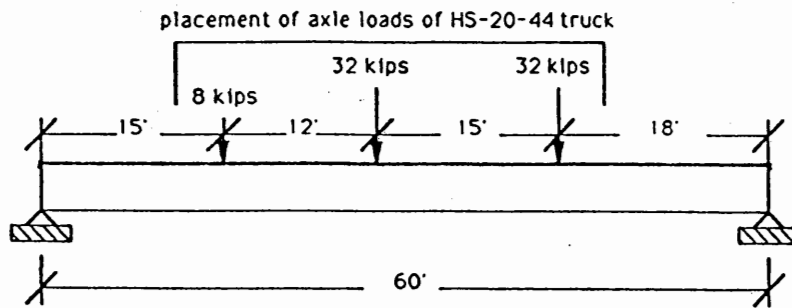


(b)

Figure 21. Secondary Deck Forces with Reduced Stiffness, (a) Secondary Moment, (b) Secondary Shear

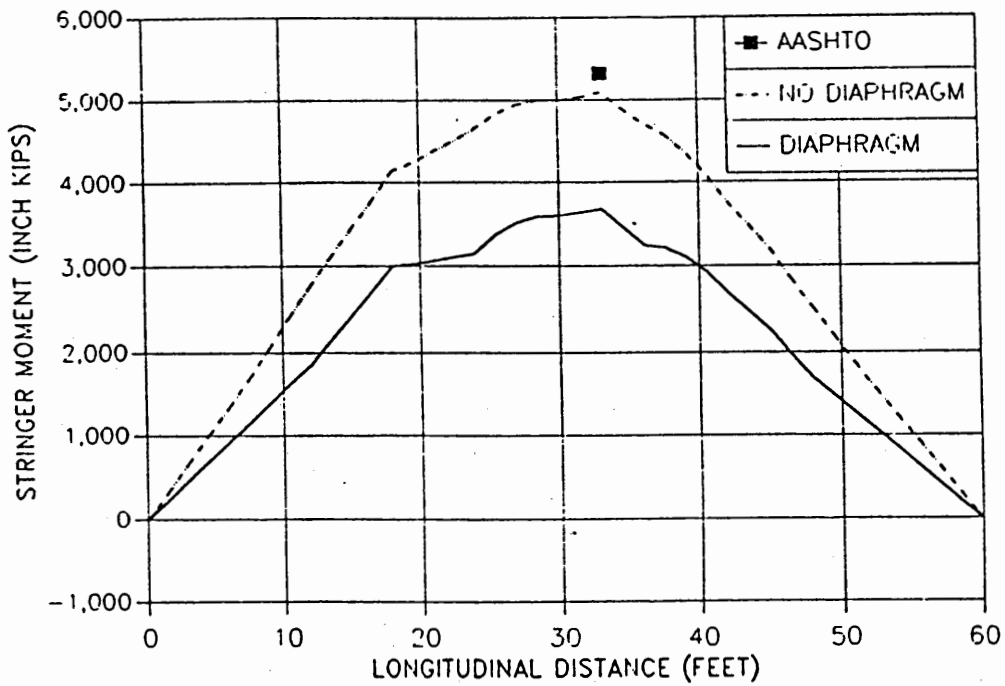


END VIEW OF THE BRIDGE

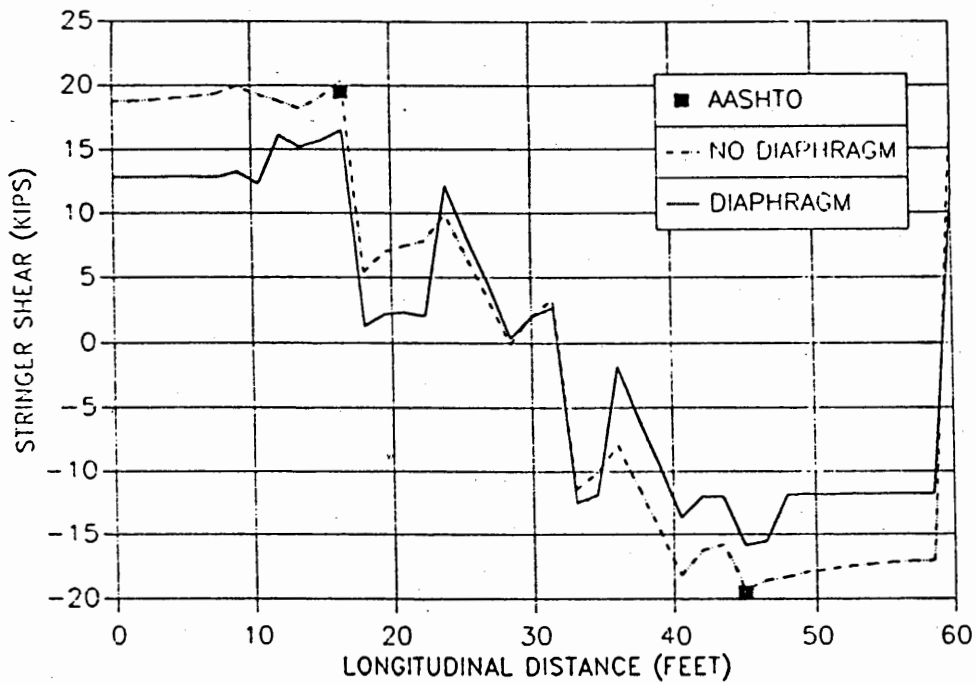


SIDE VIEW OF THE BRIDGE

(b)
 Figure 22. Truck Load Position, (a) Position to Produce Maximum Moment, (b) Position on Finite Element Model



(a)



(b)

Figure 23. Stringer Forces Under Wheel Load, (a) Moment Diagram, (b) Shear Diagram

values from the FE model without diaphragms. As expected, the stringer moment and shear decrease for the model with diaphragms. This is due to better transverse load distribution when diaphragms are included.

The improved transverse distribution of load caused by the diaphragms can be illustrated by applying a single wheel load (16 kips) at one edge of the bridge at midspan. The transverse deflection given by the FE model for the bridge with and without diaphragms is shown in Figure 24, which clearly demonstrates this effect. More importantly, the diaphragms give better transverse distribution of the deck and stringer forces. Figure 25 shows the improved transverse distribution of the primary deck moment caused by the diaphragms. Figure 26 shows the moment and shear diagrams for the stringer on the side of the bridge opposite of the wheel load. Without diaphragms, this stringer carries very little load.

From the FE model, it was also possible to find the forces in the diaphragm members. For all cases tested, it was found that the maximum stress in the diaphragm members (2 ksi) was significantly less than the allowable stress for steel. For the type of timber bridge considered, it appears that the diaphragms do not have to be designed from a strength viewpoint, but rather they should be designed to provide a desired transverse stiffness for the bridge. Additional results from this study can be found in reference [4].

5.0 Conclusions

From laboratory tests performed on several laminated timber deck specimens, the following conclusions are drawn:

1. The stiffness of a dowelled or bolted deck is only slightly greater than the stiffness of the dowels.
2. The stiffness of the stressed decks increases as the tensioning force is increased.
3. For the stressed decks, the value at which interlaminar tension begins was found to have no practical significance.
4. For the dowelled and stressed decks, the stiffness is significantly below the stiffness of a solid wood section with the same dimensions. An average stiffness of 20% of the wood stiffness was considered more realistic for laminated timber decks.
5. The stressed decks require much less steel and many

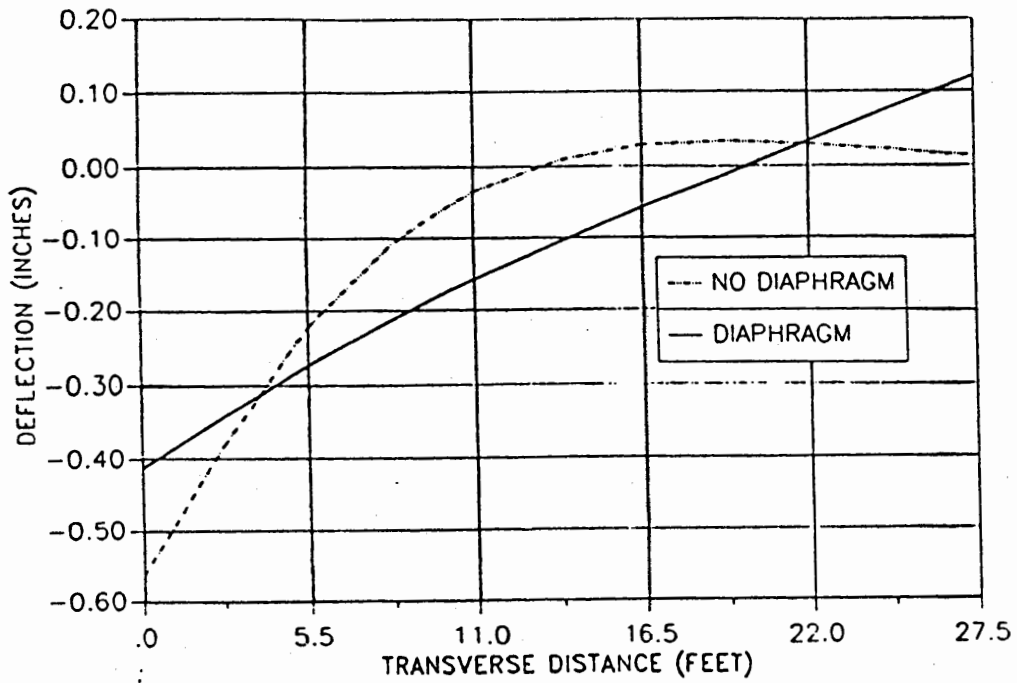


Figure 24. Transverse Deflection of the Bridge with and without Diaphragms

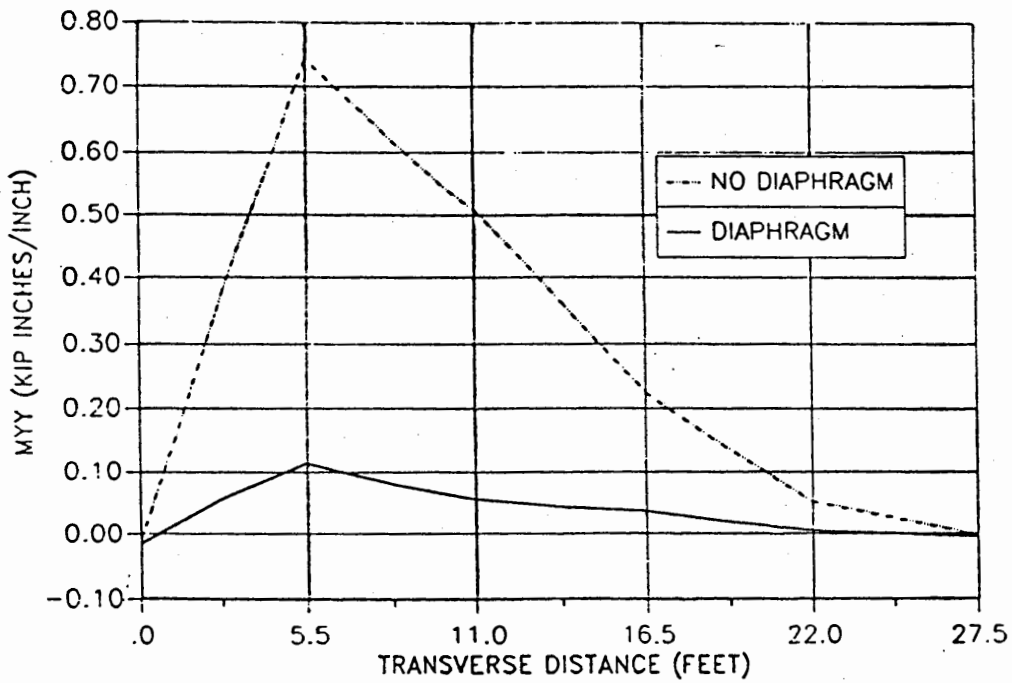
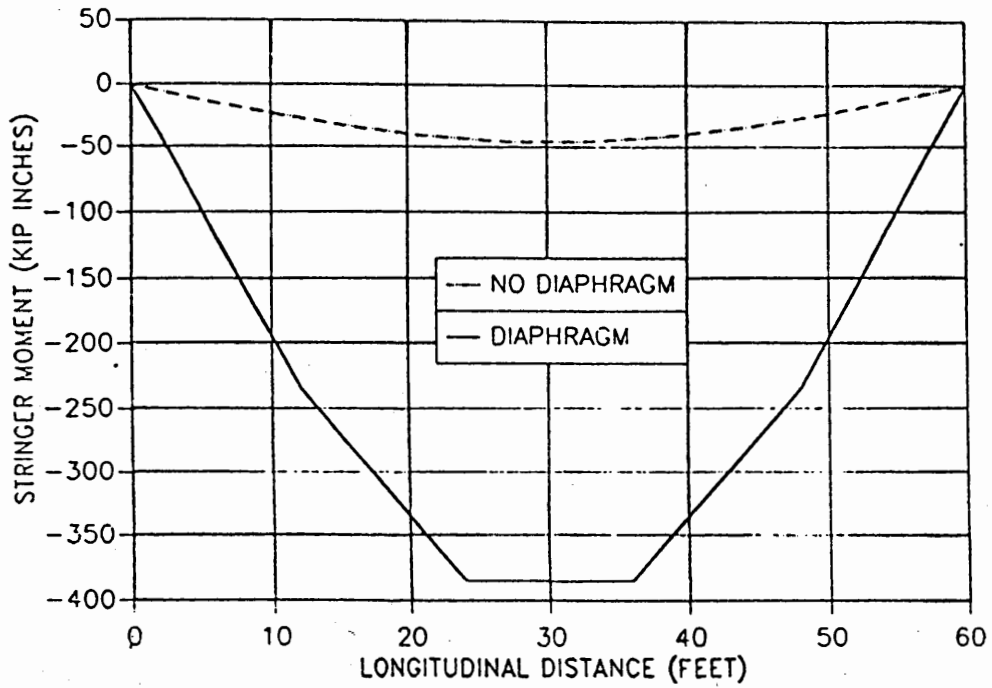
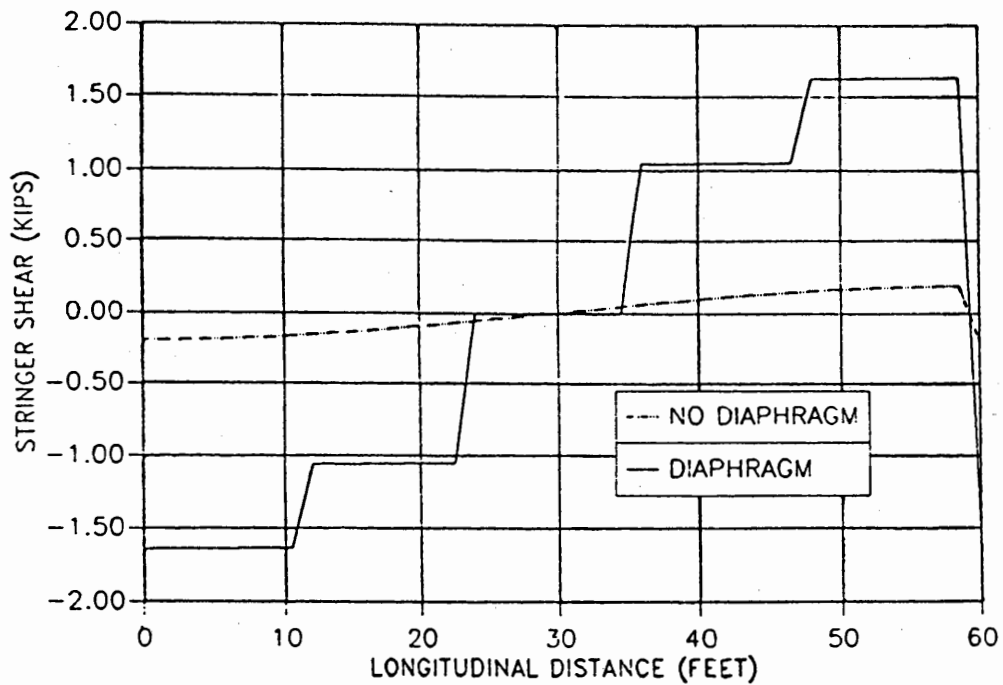


Figure 25. Primary Deck Moments with and without Diaphragms



(a)



(b)

Figure 26. Stringer Forces Opposite of Wheel Load, (a) Moment Diagram, (b) Shear Diagram

fewer holes to be drilled than the dowelled deck, and therefore are expected to be more economical. The stressed decks are also expected to be easy to construct.

6. The stressed deck using prestressing cable performed similarly to the stressed deck using Dywidag rods. It is expected that the loss of prestress due to creep will be significantly less for the cables. It is also expected that the cables will be more economical and easier to use for construction.

From laboratory tests performed on a small scale model of the bridge, the following conclusions are drawn:

1. The diaphragms significantly increase the transverse stiffness of the bridge. To achieve this increase in stiffness, the diaphragm connections must be rigid.
2. The agreement between laboratory tests and the finite element predictions was good.

From an analytical study performed on a proposed full scale bridge, the following conclusions are drawn:

1. The difference between composite and noncomposite behavior in both the longitudinal and transverse directions is small.
2. A two-dimensional finite element model can be used to model the noncomposite behavior of a three-dimensional bridge by using an appropriate "diaphragm element".
3. The FPL results for deck forces do not agree well with the finite element model results.
4. The difference in the secondary deck forces using thin and thick plate theories is significant.
5. Reducing the longitudinal deck stiffness to a more realistic value significantly affects the deck forces.
6. AASHTO values for maximum stringer moment and shear agreed well with the finite element model without diaphragms. The presence of diaphragms results in better transverse load distribution, and significantly reduces the maximum moment.
7. The maximum stress in the diaphragm members was found to be much less than the allowable stress for steel. Design of diaphragms should be based on obtaining a desired transverse bridge stiffness.

References

1. Guide Specifications for the Design of Stressed-Laminated Wood Decks, American Association of State Highway Officials, Washington, DC, 1991.
2. Ritter, M.A., "Timber Bridges: Design, Construction, Inspection, and Maintenance," USDA Forest Service, Washington, DC, 1990.
3. Sarisley, E.F. and M.L. Accorsi, "Prestress Level in Stress-Laminated Timber Bridges," ASCE Journal of Structural Engineering, 116(11), 3003-3019, 1990.
4. Anderson, S.T., "Analytical and Experimental Study of Timber Bridges Comprised of Longitudinal Stringers, Transverse Decking, and Diaphragms," Masters Thesis, University of Connecticut, 1992.
5. Standard Specifications for Highway Bridges, 13th Ed., American Association of State Highway Officials, Washington, DC, 1983.
6. McCutcheon, W.J. and R.L. Tuomi, "Procedure for Design of Glued-Laminated Orthotropic Bridge Decks," USDA Forest Service, Madison, Wisconsin, 1973.
7. McCutcheon, W.J. and R.L. Tuomi, "Simplified Design Procedure for Glued-Laminated Bridge Decks," USDA Forest Service, Madison, Wisconsin, 1974.
8. Taylor, R.J. and P.F. Csagoly, "Transverse Post-Tensioning of Longitudinal Laminated Timber Bridge Decks," Transportation Research Record, 665, 236-244, 1978.

Appendix A: Timber Bridge Design

Bridge Configuration: span $L=60$ ft, width $W=27$ ft 6 in
Loading Criteria: HS 20-44 live load, 3 in asphalt surface
Materials: glued laminated stringers (SYP or DF, 24F-V3,V4)
 laminated eastern hemlock deck

Interior Stringer Design

Assume: 6 stringers at 5 ft 6 in o.c.
 12-1/4 in x 45 in stringers (DF)
 or 10-1/2 in x 49-1/2 in stringers (SYP)
 6-3/4 in thick deck
 weight of timber = 50 pcf (AASHTO 3.3.6)
 weight of asphalt concrete=150 pcf (AASHTO 3.3.6)

Dead Load per Stringer:

deck = $(6.75)(50)(5.5)/12 = 154.7$ plf
asphalt = $(3)(150)(5.5)/12 = 206.3$ plf
stringers = $(12.25)(45)(50)/144 = 191.4$ plf (DF)
 = $(10.5)(49.5)(50)/144=180.5$ plf (SYP)
total dead load = 552.4 plf

Bending:

dead load moment = $(.552)(60)^2/8 = 248.6$ kip-ft
live load moment, truck load controls
HS20-44, from AASHTO Appendix A
 $M_{LL}/\text{lane} = 806.5$ kip-ft
DF = $s/5.0 = 5.5/5.0 = 1.1$
 $M_{LL} = (806.5)(1.1)/2 = 443.6$ kip-ft
total moment = 692.2 kip-ft

Section Properties:

stringers:	stringers:
12-1/4 in x 45 in	10-1/2 in x 49-1/2 in
size factor = .863	size factor = .854
section modulus = 4134 in ³	section modulus = 4288 in ³
actual bending stress =	actual bending stress =
$(692.2)(12000)/4134=2009$ psi	$(692.2)(12000)/4288=1937$ psi

design value in bending ($C_M=1.0$, dry condition)

$F_{bx}' = (2400)(.863)(1.0) = 2071 > 2009$
 $F_{bx}' = (2400)(.854)(1.0) = 2050 > 1937$

Shear:

total dead load = 552.4 plf

V_{DL} @ depth of stringer from support = $(.552)(60/2 - 45/12)$
= 14.5 kip

maximum reaction = 30.4 kip per wheel line
(AASHTO Appendix A)

$V_{LL} = (.5)[(.6)(30.4)+(1.1)(30.4)] = 25.8$ kip

total shear = 40.3 kip

for SYP $A=519.8$ in², and for DF $A=551.2$ in²
actual shear stress = $(1.5)(40.3)(1000)/(519.8) = 116$ psi
design value for shear ($C_M=1.0$) SYP $F_{vx}'=200$ psi > 116
(AASHTO Table 13.2.2A)

DF $F_{vx}'= 165$ psi > 116

Overload Provisions: does not apply for HS 20-44 load
(AASHTO 3.5.1)

Deflection: ($C_M=1.0$)

from Ritter Table 16-8,
deflection coefficient = 2.45×10^{11} lb in³

for SYP: $E = 1.8 \times 10^6$ psi, $I = 106126$ in⁴
for DF: $E = 1.8 \times 10^6$ psi, $I = 93023$ in⁴

live load deflection
 $(2.45 \times 10^{11})/[(1.8 \times 10^6)(93023)] = 1.46$ in < $L/360$

Camber for Dead Load:

dead load deflection
 $[(5)(552.4/12)(60 \times 12)^4]/[(384)(1800)(93023)] = .96$ in

for creep (Ritter) use $(1.5)(.96) = 1.5$ in

Area for Bearing:

R_{DL} at support = $(.552)(60/2) = 16.6$ kips

maximum reaction = 30.4 kip per wheel line
(AASHTO Appendix A)

$R_{LL} = (1.1)(30.4) = 33.4$
total reaction = 50 kip

assume wet use for bearing ($C_M = .667$)
design value for bearing = $(.450)(.667) = .300$ ksi

area for bearing = $(50)/(.300) = 167$ in²

bearing length:

for SYP $(167)/(10.5) = 16$ in,

for DF $(167)/(12.25) = 14$ in

Doweled Deck Design

Basic design equations: (AASHTO 3.25.1.3)
using $t = 6.75$ in

s = clear span + half stringer width
= $53.75 + (10.5/2) = 59$ in (controls)
 s = clear span + deck thickness = 60.5 in

primary moment

$M_x = (16)[.51 \log(59) - .51] = 6.3$ kip in/in

$F_b = 1450$ psi (AITC, #2 Hemlock)

assume dry $C_M = 1.0$, and $C_F = (12/6.75)^{1/9} = 1.07$

$t = (6 M_x / F_b)^{1/2} = [(6)(6300) / (1.07)(1450)]^{1/2} = 4.94$ in

primary shear

$R_x = .034 P = .034 (16) = .544$ kip/in

$F_v = 85$ psi

$F_v = 2 \times 85 = 170$ psi for no splits in timber
(AASHTO Table 13.2.1A, footnote h)

$t = (3 R_x / 2 F_v) = (3)(544) / (2)(85) = 9.6$ in

$t = (3)(544) / (2)(170) = 4.8$ in

use $t = 5$ in

deck deflection (FPL report, Figure 17)

$a/s = .333$, $b/a = .75$, $P = 16$ kip, $E = 1100$ ksi

(#2, Eastern Hemlock)

deflection = $.18$ in ($.18$ in = $s/360$)

dowel design

$s = 59$ in

$R_{TY} = P (s-20) / (2 s) = 5288$ lb

$M_{TY} = P [s (s-30)] / [20 (s-10)] = 27935$ lb in

try 1.5 in diameter dowels

$R_D = 2770$ lb, $M_D = 8990$ lb in

$n = (1000/1000) [(5288/2770) + (27935/8990)] = 5.02$

use 5 dowels per bay

dowel stress = $1/n (C_R R_{TY} + C_M M_{TY}) = 20162$ psi < 36000 psi

Stressed Deck Design

For primary moment and shear, use deck thickness $t=5$ in (same as dowelled deck).

Design prestress system using same secondary moment and shear.

required prestress

Assume secondary moment and shear are uniform across bay

$$V_T = (5288)/(66) = 80.1 \text{ lb/in,}$$

$$M_T = (27935)/(66) = 423.3 \text{ lb in/in,}$$

$$u=.45$$

$$\text{opening due to bending: } p = 6 M_T/t^2 = 101.6 \text{ psi}$$

(AASHTO 13-20) (controls)

$$\text{slipping due to shear: } p = (1.5 V_T)/(u t) = 53.4 \text{ psi}$$

(AASHTO 13-23)

$$\text{initial prestress } p_i = 2.5 (101.6) = 254 \text{ psi} < 550 \text{ psi}$$

(comp. per. to grain)

area of prestress rod

$$f_s = 0.8 (150) = 120 \text{ ksi for initial,}$$

$$\text{and } f_s = 0.7 (150) = 105 \text{ ksi after losses}$$

$$\text{use } s = 66 \text{ in (rod spacing)}$$

(does not meet AASHTO specification)

$$A = p_i s t / f_s = .7 \text{ in}^2, \text{ use 1 in diameter rods (A=.78 in}^2)$$

(AASHTO 13-26)

$$A > .0016 s t = .53 \text{ in}^2 \text{ (does not meet AASHTO 13-27)}$$

area of prestress cable

$$f_s = 0.8 (270) = 216 \text{ ksi for initial,}$$

$$\text{and } f_s = 0.7 (270) = 189 \text{ ksi after losses}$$

$$\text{use } s = 66 \text{ in (rod spacing)}$$

(does not meet AASHTO specification)

$$A = p_i s t / f_s = .39 \text{ in}^2 \text{ (AASHTO 13-26)}$$

$$A < .0016 s t = .53 \text{ in}^2 \text{ (AASHTO 13-27)}$$